In presenting the dissertation as a partial fulfillment of the requirements for an advanced degree from the Georgia Institute of Technology, I agree that the Library of the Institution shall make it available for inspection and circulation in accordance with its regulations governing materials of this type. I agree that permission to copy from, or to publish from, this dissertation may be granted by the professor under whose direction it was written, or, in his absence, by the dean of the Graduate Division when such copying or publication is solely for scholarly purposes and does not involve potential financial gain. It is understood that any copying from, or publication of, this dissertation which involves potential financial gain will not be allowed without written permission.

THROUGH-FLOW DRYING OF TUFTED TEXTILE MATERIALS

A THESIS

Presented to

The Faculty of the Graduate Division

by

James Donald Brock

In Partial Fulfillment

of the Requirements for the Degree

Master of Science in Mechanical Engineering

Georgia Institute of Technology

June, 1963

THROUGH-FLOW DRYING OF TUFTED TEXTILE MATERIALS

Approved:

Date approved by Chairman: 5/8/63

ACKNOWLEDGMENTS

The author acknowledges with pleasure the help, support, and encouragement given him by his advisor, Dr. Charles W. Gorton. Many valuable suggestions were also contributed by Professor H. G. Rylander, especially in the design of the test equipment.

The assistance of Professor Kenneth Purdy, Mr. John Davis, and Mr. Lewis Cavalli in assembling the test stand was also greatly appreciated.

Particular thanks are due to Singer-Cobbie, Inc., for furnishing the test samples and to the Department of Mechanical Engineering for the use of its equipment during the investigation.

TABLE OF CONTENTS

TABLE OF CONTENTS (Continued)

LIST OF TABLES

LIST OF ILLUSTRATIONS

LIST OF ILLUSTRATIONS (Continued)

LIST OF SYMBOLS

a - number of rows of backing yarn in direction of tuft rows per inch

A - cross-sectional area of sample

A_f - cross-sectional area occupied by fiber

A_o - open cross-sectional area

A_s - interfacial surface area

A_{so} - cross-sectional area of single opening

b - number of rows of backing yarn per inch in a direction perpendicular to the tuft rows

C_f - the coefficient of drag through the material

c_p - specific heat of air

d_f - yarn diameter

d_h - hydraulic diameter of flow channels through material

$D_{\mathcal{V}}$ - mass diffusivity

g_c - constant, 32.174 lb. force-foot/lb. mass-sec.^{2}

h - thickness of carpet in direction of flow

$\bar{h}_c$ - average convective heat transfer coefficient

h_d - convective mass transfer coefficient

k - thermal conductivity of air

m - weight of dry material

m_w - weight of water in material

M - moisture content defined as weight of water per unit weight of dry material

M_c - critical moisture content

LIST OF SYMBOLS (Continued)

M_e - equilibrium moisture content

n - number of rows of tuft per inch

N - cotton yarn number

N_o - number of openings

P_a - partial pressure of dry air based on upstream conditions

P_v - partial pressure of water vapor

P_w - wetted perimeter of opening

Pr - Prandtl number

ΔP - pressure drop across the material

Q - flow rate through material

R_a - gas constant for air

Sc - Schmidt number

$S.G.$ - specific gravity of fiber

t - time

t_c - elapsed time when falling rate period starts

T_1 - air temperature upstream to sample

T_d - dry bulb temperature of room air

T_w - wet bulb temperature of room air

V - velocity of air flow through the material

W - width of single opening

W_b - weight of backing per unit area

α - slope of straight line approximating falling rate curve

ρ_m - density of air-water vapor mixture

LIST OF SYMBOLS (Continued)

μ - dynamic viscosity of air

ω - humidity ratio of air at differential section in material

ω_1 - humidity ratio of air upstream to sample

ω_2 - humidity ratio of air downstream to sample

ω_s - saturation humidity ratio corresponding to adiabatic saturation temperature of upstream air

ω_w - humidity ratio of air at the wall of the drying substance

SUMMARY

It was the purpose of this investigation to study the through-flow air drying of tufted carpet. Since this was an entirely new concept of drying in the tufted carpet field, it was necessary to determine the variables which affected the drying rates and drying times required for various materials.

The experimental data for the investigation was obtained in a special constructed wind-tunnel dryer which was equipped with electronic controlling and measuring instruments. The tunnel was capable of drying under predetermined temperature (room to 300° F.) and velocity (0 to 2000 fpm).

The experimental pressure differential and flow rate data was grouped into two dimensionless parameters (a Reynolds number and a drag coefficient) which could be fitted to a single curve. The drag coefficient was used to analytically predict the drying rate during the unbound moisture region of drying. This constant drying rate was then used in an approximate analytical solution for determining the drying time during the falling rate period.

Using these equations and the critical moisture content for the material, the total drying time was predicted.

It was found that the drying time decreased with increasing air temperature, decreasing humidity ratio and increasing flow rate. It was also found that tufted carpet exhibited all regions of the rate-of-drying curve. The pressure differential across the carpet was found to vary linearly with the velocity for velocities in the range 250 to 900 fpm.

In conclusion, it was found that tufted carpet could be dried with through-flow drying in less than one-fifth the time required in present industrial dryers. The practical limitation of this type of drying was also briefly discussed.

CHAPTER I

INTRODUCTION

Present industrial carpet dryers are essentially classified according to the method used in conveying the material through the dryer, such as a tenter or loop. These classifications give little indication of the type of air flow principle used, which is of prime importance when determining drying rates. The highest production units today seem to utilize an air impingement principle in which air is forced through horizontal ducts above and below the carpet. The air leaves the ducts at high velocities through orifice-like holes and strikes the carpet. The problem in this investigation developed as a result of preliminary drying test in which air was forced through carpet, allowing more air to contact more drying surfaces and, thus, increased diffusion rates.

Problem

In order to set up drying schedules and to determine the size of equipment for drying of tufted carpet, it is necessary to know the time which will be required to dry various tufted materials from one moisture content to another under specific conditions. The estimate of the influence that different drying conditions will have upon the

time for drying will also be considered for through-flow drying. The particular emphasis in this investigation will be on drying of tufted wool and nylon carpets. The knowledge of the mechanism of drying is so incomplete that it is necessary, with few exceptions, to rely on at least some experimental measurements for these purposes (16)*.

Purpose

It is, therefore, the purpose of this investigation to analytically predict the drying rates in the unbound moisture region and falling rate period** and to experimentally verify these rates and the total drying time for various tufted materials for through-flow drying. It is also proposed to determine dimensionless groups of variables which affect the drying rates and to experimentally obtain curves relating these groups. By momentum-heat-mass transfer analogies these curves will be used to determine the convective heat and mass transfer coefficients for forced convection air flow through tufted carpet. These coefficients will then be used to predict the drying time along with the drying rates in the unbound moisture region and falling rate period.

---

*Numbers in paraentheses refer to the references listed in the Bibliograph, Appendix G, page 95.

**See Chapter II, page 5, for definitions.

Use

In 1961, 175 million square yards of tufted rugs and carpets were produced in the United States, having a monetary value of 517.7 million dollars. In this production approximately 300 million pounds, 150,000 tons, or 36 million gallons of water had to be removed in various types of industrial dryers. This number does not include the over 400,000 additional tons which were removed by vacuum extractors, prior to entering the dryer.

Drying times of from 5 to 40 minutes are now required in present industrial dryers. The sizes of these units range in lengths of from 40 to 150 feet, widths from 15 to 30 feet and heights from 4 to 12 feet. Hence the development and investigation of a method of drying which greatly reduces this drying time and the dryer size are of great practical importance.

CHAPTER II

BACKGROUND

Mechanism of Drying

The term "drying" refers to the removal of moisture from a substance. This may be done by evaporation of the moisture either into a gas stream or without a gas to carry the moisture away, but the mechanical removal of such moisture by extraction or centrifuging is not ordinarily considered as drying (16). In this brief discussion the moisture will be considered as water and the gas as air, although the techniques and relationships explained here will be equally applicable to other systems as well.

When a wet substance is continually exposed to a stream of gas having a fixed temperature and humidity, the substance will either lose or gain moisture until it reaches some equilibrium state. This equilibrium state is referred to as the equilibrium-moisture content* at the prevailing conditions and depends on the substance geometry, contact surface, and composition as well as the gas stream properties and conditions.

To assist in the explanation of the regions of dry-

---

*Moisture content is defined as lb. moisture per lb. dry substance.

ing, a typical equilibrium-moisture curve is shown in Figure 6, page 49. Considering the curve, if the substance were exposed to a steady stream of air having a relative humidity of A, it would lose or gain moisture until its equilibrium concentration corresponding to point "D" on the curve was eventually reached. Further exposure to the air would not affect the moisture content of the substance. From this observation, it is seen that the final state of dryness which can be reached depends on the prevailing conditions of the air stream and could be reduced only by reduction in the air humidity. The moisture contained in the substance up to a concentration corresponding to point "C" on the curve exerts a vapor pressure below the saturation pressure of water vapor at the same temperature and is referred to as "bound moisture." This moisture is held in small capillaries or crevasses inside cell walls of the structure in solution throughout the solid, and by chemical or physical absorption on substance surfaces. The moisture in or on the substance to the right of point "C" is referred to as unbound moisture and exerts an equilibrium vapor pressure equal to that of pure water at the prevailing temperature. The free moisture, as shown in Figure 6, is the moisture contained by a substance in excess of the equilibrium moisture. Only this moisture can be evaporated and, as previously stated, its lower limit depends on the upstream air conditions.

For explanation of the drying rates associated with the regions of drying described above, refer to Figure 7, page 50. Upon exposure to a gas stream, the surface temperature of a substance will begin to adjust to some equilibrrium temperature corresponding to the wet bulb temperature of the air stream, t_s. During this adjustment, if the surface temperature is lower than t_s, the drying rate will increase as shown in portion A B on the curve. If the surface temperature is higher than t_s, the drying rate will decrease as shown in period A'B. The time required for this period of adjustment is usually short and is often neglected in calculations of drying time.

The portion B C on the curve represents the removal of the unbound moisture. During this period a balance between heat transfer and mass transfer from the surface occurs and a constant temperature and humidity ratio at the surface results. This leads to a constant drying rate during this period which depends on the heat and mass transfer coefficients and the corresponding gradients associated with these; i.e., the rate depends on the rate of diffusion of water vapor through the surface air film out into the main body of air, or more generally the humidity, temperature and air velocity.

Point "C" on the curve in Figure 7 refers to the critical moisture content. Below this point, portion C D, the surface film of moisture is reduced to the point that

further drying will cause dry spots to appear; i.e., the vapor pressure is below saturation at the surface. This causes the drying rate to decrease. This is the first part of the falling rate period and is referred to as unsaturated surface drying. Upon reaching point "D," the surface is completely dry. In certain drying operations this portion of the curve is completely missing.

On continued drying, the portion of the curve D E in Figure 7 appears. In this region the rate of drying is largely dependent of the rate of diffusion of moisture from within the body to the surface; therefore, further reduction of the drying rate occurs. This is the second part of the falling-rate period and is the least understood and most complex region of drying. According to Sherwood (14) in this zone, the curves are apparently always of the same shape, concave upwards when rate of drying is plotted against water content. Sherwood states that it can be shown that the drying in this zone is controlled by the rate of internal diffusion, by noting that variations in humidity or air velocity do not affect the rate. Secondly, the rate is inversely proportional to the slab thickness; whereas, in surface drying or evaporation the rate of drying is independent of the thickness and varies with humidity and air velocity. More recent reports of different materials indicate that the rate in the second zone is inversely proportional to the square of the slab thickness. According to

Carrier (3), the air temperature and conduction of heat into the material affects the rate of diffusion, since the vapor pressure of the internal moisture increases with the temperature.

Review of Related Literature

The pioneer statements regarding drying were published by Lewis (7). About the same time Carrier (3) presented a theory of evaporation from a thermodynamic standpoint and also pointed out how chemical and physical behavior of the material being dried affects the drying rates. Several papers by Sherwood and his co-workers (13, 14, 15) further extended the understanding of the mechanism of drying of solids by an explanation of the propagation of moisture through a solid during drying. Newman (11) proposed theoretical equations for the moisture distribution during drying. The work of these early investigators, however, was not universally applicable to all substances since geometries, capillary forces, and contact surfaces vary with each material.

Many noteworthy contributions to the air drying of particular substance have been reported but due to the complexity and scope of the field only contributions related to the drying of textile fibers will be considered here.

When the temperature or moisture content of air flowing through a mass of textile fibers is changed, changes in

the temperature and moisture content are propagated through the fibers. Cassie and Baxter (4, 5) have investigated this process for sudden changes in air temperature or concentration and Cassie has developed a theory for the propagation. The theory predicts that the propagation takes place in two fronts, fast and slow, moving with constant velocities through the mass. The fast front is associated with the temperature and the slow front with the moisture content. This theory considers that equilibrium is established between the fibers and air directly after passage of the front. McMahon and Downes (10) took in account the finite rate in which equilibrium is established. They present an analysis of the effect which a finite rate of approach to moisture equilibrium between a fiber and its surrounding has on the mode of propagation of changes through the mass of fibers. They show, as did Cassie, that a constant-velocity-wave solution for the propagation of changes through a mass exists during drying. This solution was developed for a bed of wool fibers but is applicable also to thinner layers such as those of tufted textile carpets. The solution of the wave equation required the experimental determination of a plot similar to Figure 6 to determine the propagation of changes. In these approaches experimentally determined rate constants were used to calculate the drying rates.

Bell and Grosberg (1) obtained a solution for the first part of the falling rate period of drying of thick

textile materials which should apply equally well to thinner structures although experimental verification was not given in their presentation. Bell showed that during the falling rate period, textile structures consist of a central core containing liquid water, the outer surface being dry. McCready and McCabe (9) analyzed the heat and mass transfer between the wet core and the air stream. The temperature of the wet core depended on the relative resistance of the layer of dry material and of the boundary layer to diffusion and heat conduction. Bell calculated this resistance and determined the core position by the condition within the core. Knowing the temperature and position of the core boundary, he was able to predict the falling rate curve.

Perry (12) suggested an approximate analytical solution for the falling-rate period which is applicable to essentially any material. In this approach, the falling-rate period is approximated as a straight line between the critical moisture content and the equilibrium moisture content.

Utilizing the most applicable of the above approaches, the rates of the complete drying curve can be predicted analytically and the drying time could be predicted if the critical moisture content was known. Unfortunately, none of the above-listed references give any insight on the magnitude of the critical moisture content. The analytical

solution to this problem is still to be solved before an analytical prediction of the drying time can be given.

CHAPTER III

THEORY

Pressure Drop

The following are considered as the significant variables which affect the pressure drop through tufted carpet:

1. upstream air temperature
2. air flow rate
3. moisture content of carpet
4. density of fiber
5. weight of carpet (lbs. per sq. ft.)
6. weight and weave of backing

The correlation of these variables will be made with a dimensionless Reynolds number, based on the open area and a drag coefficient, based on the pressure drop across the material. In the derivation the following assumptions will be made:

1. The carpet will be considered as consisting wholly of the tufted fiber.
2. The resistance to air flow will be considered to be most significant through the backing with the tufted fiber adding resistance by causing additional rows of fibers or a closer weave.

3. The air-water vapor mixture will be considered as a perfect gas.
4. The water contained in the backing will be considered as being within the yarn and not of sufficient magnitude to enlarge the fiber diameter.
5. The viscosity of the air-water vapor mixture will be considered as being that of air at the same temperature.

The derivation of the Reynolds number is as follows:

$$Re = \frac{Q\, d_h\, \rho_m}{A_o\, \mu} \qquad (1)$$

Where: Q = flow rate of air through the material

d_h = hydraulic diameter

ρ_m = density of air-water vapor mixture

A_o = average open air through the carpet

μ = viscosity of air-water vapor mixture

The average open area (A_o) will be determined as follows:

$$A_f = (a + b + n)d_f \qquad (2)$$

Where: A_f = area occupied by the fibers per square inch

a = number of backing rows per inch in direction of tuft rows

b = number of backing rows per inch in perpendicular direction to tuft rows

n = number of rows of tufts per inch

d_f = yarn diameter, inches

The yarn diameter is determined as follows:

$$d_f = \frac{0.0438}{\sqrt{N \times S.G.}} \tag{3}$$

Where: N = the cotton yarn number defined as the yards of fiber per pound divided by 840 which is the standard for No. 1 cotton

S.G. = specific gravity of fiber

The cotton yarn number for the backing is determined as follows:

$$N = \frac{(a + b)}{W_b} \tag{4}$$

Where: W_b = the weight of backing in lbs. per square inch

The open area is:

$$A_o = A - A_f \tag{5}$$

Where: A_o = open cross-sectional area, square inches

A = unit cross-sectional area of sample

In this analysis, the portion of the fibers which crossed over other fibers in the woven material is neglected due to the porosity of the material. The tufted fiber is considered as having the same diameter as the backing material in the calculation, since the unexposed area which they

blocked is equivalent to that of a single row of backing fiber per row of tufts.

The hydraulic diameter is defined as the cross-sectional through-flow area divided by the wetted perimeter. In this investigation the following approach correlated well with the data, although the approach was not put to a severe test with the range of carpet samples tested.

$$d_h = \frac{A_{so}}{P_w}$$

Where: A_{so} = cross-sectional area of single opening

P_w = wetted perimeter of opening

Considering the openings as squares,

$$d_h = \frac{W^2}{4W} = \frac{W}{4}$$

Where: W = width of opening

or

$$d_h = \frac{\sqrt{A_{so}}}{4} \qquad (6)$$

The number of openings is calculated as follows:

$$N_o = a(b - n) \qquad (7)$$

Where: N_o = the number of openings

Since $$A_{so} = \frac{A_o}{N_o}$$

$$d_h = \frac{\sqrt{A_o}}{4\sqrt{a(b-n)}} \tag{8}$$

The density of the air-water vapor mixture is determined as follows:

$$\varrho_m = \frac{(1+\omega)P_a}{R_a T_1}$$

Where: P_a = partial pressure of dry air based on upstream conditions

ω = humidity ratio (lbs. water vapor per lb. dry air)

R_a = gas constant for air

T_1 = upstream air temperature

For an air-water vapor mixture, the humidity ratio is given by:

$$\omega = 0.622 \frac{P_v}{P_a}$$

Therefore:

$$\varrho_m = \frac{P_a + 0.622\ P_v}{R_a T_1} \tag{9}$$

Where: P_v = partial pressure of the water vapor in the mixture

Substituting equations (8) and (9) into equation (1)

$$Re = \frac{Q(P_a+0.622\ P_v)}{4\mu R_a\ T_1 \sqrt{A_o a(b-n)}} \tag{10}$$

The derivation of the drag coefficient is as follows:

$$C_f = \frac{\Delta P}{\rho_m\ V^2/2g_c} \tag{11}$$

Where: C_f = the coefficient of friction or drag coefficient of the material

ΔP = the pressure drop through the material

V = volume flow rate divided by the open area

g_c = 32.174 lb. mass foot/lb. force, sec.

Rewriting

$$C_f = \frac{2g_c\ \Delta P\ A_o^2}{\rho_m\ Q^2} \tag{12}$$

Substituting equation (9) into equation (12)

$$C_f = \frac{2g_c\ \Delta P\ A_o^2\ R_a\ T_1}{Q^2(P_a+0.622\ P_v)} \tag{13}$$

Initial Adjustment

Due to the complexity of this period of drying, it will not be considered in this analysis. The variation in open area and, therefore, the velocity of air flowing through the material added to the difficulty. In drying of carpet from an initial moisture content of 200 per cent or less, the time in this period is usually negligible in comparison with the other periods of drying.

Constant Rate Period

Since the mechanism of mass, heat, and momentum transfer are closely related, the data taken for one transfer operation is useful in predicting the rate of transfer in other operations. The interrelation of heat and momentum transfer, usually referred to as the Reynolds analogy, results in the following relation for fluids having a Prandtl number equal to one.

$$\frac{\bar{h}_c}{c_p \rho_m V} = \frac{C_f}{2} \left(\frac{A_o}{A_s} \right) \qquad (14)$$

Where: $\bar{h}_c$ = average convective heat transfer coefficient

c_p = specific heat of air

A_s = interfacial surface area

Modifying equation (14) to comply with experimental results for Prandtl numbers different from one. According to Kreith

$$\frac{\bar{h}_c}{C_p \rho_m V} = \frac{c_f}{2} \left(\frac{A_o}{A_s} \right) P_r^{-2/3} \qquad (15)$$

Where: Pr = Prandtl number

Following Kreith (6) using a similar approach for mass transfer with the following assumptions:

1. Water vapor is considered as the only diffusing medium.
2. Mass transfer rates are considered as low enough so that the velocity normal to the surface is small when compared to the free stream velocity.
3. The mass fraction of water is small when compared to one.

$$h_d = \left(\frac{\bar{h}_c}{c_p} \right) \left[\left(\frac{c_p \mu}{k} \right) \left(\frac{\rho_m D_{\mathcal{V}}}{\mu} \right) \right]^{2/3} = \left(\frac{\bar{h}_c}{c_p} \right) \left(\frac{P_r}{SC} \right)^{2/3} \qquad (16)$$

Where: h_d = convective mass transfer coefficient*

---

*The mass transfer coefficient is defined by the equation

$$\frac{dm_w}{dt} = h_d \rho_m (\omega_w - \omega)$$

Where: m_w = mass of water removed

ω_w = humidity ratio or mass fraction of the air-water vapor mixture at the drying surface

ω = humidity ratio of air stream flowing past the drying surface.

k = thermal conductivity of air

D_{ν} = mass diffusivity

Sc = Schmidt number

Substituting equation (15) into equation (16)

$$h_d = \frac{C_f}{2} \left(\frac{A_o}{A_s} \right) V \rho_m \left(Sc \right)^{-2/3} \qquad (17)$$

The moisture content of carpet is defined as follows:

$$M = \frac{m_w}{m} \qquad (18)$$

Where: M = moisture content

m_w = weight of water

m = total weight of dry sample

Following an approach similar to Trebal (16), the maximum rate at which moisture can be removed from a substance occurs when the air leaves the substance saturated at the adiabatic saturation temperature, with a humidity ratio ω_s.

$$\left(\frac{dm_w}{dt} \right)_{max.} = \rho_m V A_o (\omega_s - \omega_1) \qquad (19)$$

Where: t = time

ω_1 = humidity ratio of upstream air

The gas will usually leave the substance at some humidity ratio ω_2 less than ω_s.

$$\frac{dm_w}{dt} = \rho_m V A_o (\omega_2 - \omega_1) \qquad (20)$$

Considering a differential section, the air-humidity ratio will increase as it proceeds through the carpet and the air will be subjected to a change $d\omega$. The rate of drying will be

$$\frac{dm_w}{dt} = \rho_m V A_o \, d\omega = h_d \, dA_s (\omega_w - \omega) \qquad (21)$$

Dividing dA_s by the unit length in the direction of flow h and multiplying by the differential length dx, equation (21) becomes

$$\rho_m V A_o \, d\omega = h_d \frac{A_s}{h} (\omega_w - \omega) dx \qquad (22)$$

Rearranging and integrating through the material assuming h_o constant

$$\int_{\omega_1}^{\omega_2} \frac{d\omega}{\omega_w - \omega} = \int_o^h \frac{h_d A_s}{\rho_m V A_o h} \, dx$$

and

$$\ln \frac{\omega_w - \omega_1}{\omega_w - \omega_2} = \frac{h_d A_s}{\rho_m V A_o}$$

$$\frac{\omega_w-\omega_1}{\omega_w-\omega_2} = e^{h_d A_s/\rho_m VA_o} \qquad (23)$$

Rearranging equation (23)

$$\omega_2-\omega_1 = (\omega_w-\omega_1)\left[1-e^{-h_d A_s/\rho_m VA_o}\right]$$

and

$$\frac{dm_w}{dt} = \rho_m VA_o(\omega_w-\omega_1)\left[1-e^{-h_d A_s/\rho_m VA_o}\right] \qquad (24)$$

Since during the unbound moisture region, a substance exerts a vapor pressure equal to that of pure water at the same temperature, the humidity ratio at the wall of the substance will correspond to ω_s; therefore,

$$\frac{dm_w}{dt} = \rho_m VA_o(\omega_s-\omega_2)\left[1-e^{-h_d A_s/\rho_m VA_o}\right] \qquad (25)$$

or

$$\frac{dm_w}{dt} = \left(\frac{dm_w}{dt}\right)_{max}\left(1-e^{-h_d A_s/\rho_m VA_o}\right)$$

Dividing both sides by the weight of sample

$$\frac{dM}{dt} = \left(\frac{dM}{dt}\right)_{max} \left(1-e^{-h_d A_s / \rho_m V A_o}\right)$$

From equation (17)

$$\frac{h_d}{\rho_m V}\left(\frac{A_s}{A_o}\right) = \frac{C_f}{2}\left(\frac{D_v \rho_m}{\mu}\right)^{2/3}$$

Therefore,

$$\frac{dM}{dt} = \left(\frac{dM}{dt}\right)_{max} \left(1-e^{-\frac{C_f}{2}\left(\frac{D_v \rho_m}{\mu}\right)^{2/3}}\right) \qquad (27)$$

Equation (27) represents the equation for the rate of drying in the unbound moisture region. As noted from the equation, the drying rate depends almost entirely on the coefficient of drag through the material.

A comparison of experimental drying rates and those calculated from equation (27) is presented in Table 16, page 89.

Falling Rate Period

Due to several controlling mechanisms during the falling rate period, a rigorous analytical solution becomes very involved. The following approximate method as suggested by Perry (12) gives a fairly accurate expression for drying time during this region of drying.

The rate of drying can be expressed as:

$$\frac{dM}{dt} = -\alpha(M-M_e) \tag{28}$$

Where: α = slope of straight line approximating falling rate.

M_e = equilibrium moisture content.

Since

$$\left(\frac{dM}{dt}\right)_{max} = -\alpha(M_c-M_e)$$

$$\alpha = \frac{-(dM/dt)_{max}}{(M_c-M_e)} \tag{29}$$

Where: M_c = critical moisture content

The negative sign occurs in equations (28) and (29) since the rate of moisture removal is decreasing.

Substituting equation (29) into equation (28)

$$\frac{dM}{dt} = \left(\frac{dM}{dt}\right)_{max} \frac{M-M_e}{M_c-M_e} \tag{30}$$

letting $$S = \frac{M-M_e}{M_c-M_e}$$

$$\frac{ds}{dt} = \frac{1}{M_c-M_e} \frac{dM}{dt}$$

$$\frac{ds}{s} = \left(\frac{dM}{dt}\right)_{max} \frac{dt}{(M_c - M_e)} \tag{31}$$

Integrating

$$-\ln s = \left(\frac{dM}{dt}\right)_{max} \frac{t - t_c}{(M_c - M_e)} \tag{32}$$

Where: t_c = elapsed time when critical moisture content was reached

Since

$$M = \frac{m_w}{m}$$

and

$$M_e = \frac{m_{we}}{m_{we} + m} = \frac{1}{1 + \frac{m}{m_{we}}}$$

Where: m_{we} = moisture contained in the material when in equilibrium with the surrounding air.

$$m_{we} << m$$

Therefore, $M_e \approx 0$

and $$s \approx \frac{M}{M_c}$$

Substituting into equation (32)

$$t - t_c = \left(\ln \frac{M_c}{M} \right) \frac{M_c}{(dM/dt)_{max}} \qquad (33)$$

Since it would take an infinite amount of time to completely dry a substance, the samples were considered as being dry when $M = 0.05M_c$; therefore,

$$t - t_c = (\ln 20) \frac{M_c}{(dM/dt)_{max}} = 2.9957 \frac{M_c}{(dM/dt)_{max}}. \qquad (34)$$

A comparison of drying times determined from equation (34) and experimental determined values is presented in Table 16. The agreement was good.

Equations (27) and (34) can be used to analytically determine the total drying time if the critical moisture content is known. Since the critical moisture content varies with the rate of drying and thickness of material, it is very difficult to determine by an analytical approach. This is discussed in more detail in Chapter VI, page 32.

CHAPTER IV

INSTRUMENTATION AND EQUIPMENT

A wind-tunnel dryer was used in this investigation and is illustrated by a diagrammatic sketch in Figure 1, and by a photograph in Figure 2. The dryer was designed and assembled in the Mechanical Engineering Research Laboratory. It is capable of drying under predetermined conditions of temperature (room to 300° F.) and air velocity (zero to 2000 feet per minute).

The air was supplied by a New York Blower No. 152 backward curved blade fan. The flow was regulated by an opposed blade outlet damper. A flexible rubber section between the outlet damper and the transition section to the fin tube sections was used to damp out the vibrations associated with the blower. The air was heated by three No. 3024 Steelfin tube sections using steam at a maximum pressure of 150 psig. as the heating medium. The dry bulb temperature upstream of the sample, as shown in Figure 5, page 47, was controlled by a Minneapolis-Honeywell Three-Mode Electr-O-Line control unit and Electronik recorder operating with a Model 1½-800 Minneapolis-Honeywell motorized valve in the steam supply line leading to the Steelfin tube sections. The valve was driven by a M903B Actionator

motor. The steam pressure was indicated by a pressure gage. The temperature pickup for the Electronik recorder was made by three iron-constantan thermocouples located in the tunnel eight diameters from the entrance. The air temperature downstream to the sample was measured and recorded by a Minneapolis-Honeywell Electronik recorder also utilizing three iron-constantan thermocouples for the pickup.

The average velocity in the tunnel was determined by a pitot tube located seven and one-half diameters from the tube entrance. The tube was positioned in the duct to give the average velocity pressure. This was calibrated with six velocity traverses at various flow rates. The calibration was made in accordance with the Air Moving and Conditioning Association Test Code, Bulletin 210. A six-inch Trimount micro-manometer was used to measure the velocity pressure in the pitot tube and the pressure drop across the test sample. Manifolds with four pressure pickups around the tunnel were used in measuring the carpet pressure drop to insure that the average pressures were measured.

The weighing section is illustrated diagrammatically in Figure 3 and by a photograph in Figure 4. The weight change of the sample while drying was determined by the change in deflection of four one-sixteenth by one inch hot rolled steel bars acting as cantilevered beams, to which a weighing frame was attached. The deflection was measured by Baldwin-Lima-Hamilton SR-4 strain gages assembled on each

side of the bars. The duct section to which the bars were attached was insulated with two inches of Fiberglas insulation and cooling air taps were installed to keep the strain gage temperature as low as possible. The entire section was totally enclosed to prevent air leakage from the tunnel which would effect the flow readings. A removable cover above the weighing frame allowed removal of the sample after each run. Handhole plates were also installed above the bars and strain gages. The weighing section was calibrated by using known weights. The change of weight was measured and recorded on a Sanborn 150 strain recorder. A full bridge was connected to the recorder to compensate for temperature changes in the weighing section and to increase the sensitivity of the unit. The weighing section has a capacity of 30 pounds, a weight variation at maximum sensitivity of 2 pounds and a sensitivity of 0.001 pounds. The weight of the sample and check on weight change after each run was determined on a nonspring Toledo balance scale.

The differentation of the drying curve was performed with a Gerber Derivimeter, Model D-2 slope reader and checked numerically.

CHAPTER V

EXPERIMENTAL PROCEDURE

Preparation of Sample

The sample was thoroughly wetted in a reservoir of cold water, and then was allowed to drain for one minute. The sample then was folded and squeezed in a press until the moisture content had been reduced to approximately 150 per cent by weight. This procedure was eliminated in a few samples to check the initial adjustment period, when drying from high initial moisture contents. The sample was weighed when dry, when wet, and after squeezing. Following the final weighing, the material was stretched and fitted between two steel circular rings which were specifically designed to fit into the weighing frame.

Preparation of Apparatus

The Sanborn strain recorder and the Honeywell Electronik controllers and recorders were started and allowed to run 30 minutes prior to the first test. With a dry dummy sample to simulate operating conditions, the dryer was started and brought up to operating temperature and allowed to run for three minutes. During this period the blower damper was adjusted to the prescribed flow rate for

the particular run, the cooling air on the weighing section was adjusted for the temperature of the run and the duct air temperature was allowed to stabilize. The flow setting was made by adjusting the damper until the flow corresponding to the related pressure in the pitot tube was reached. This pressure was measured by the micro-manometer. The air temperature for the run was set on the Honeywell Electronik controller. The dryer was then stopped.

Test Procedure

The dummy test sample was removed from the weighing frame and the prepared sample was inserted into its position. The cover above the weighing frame was bolted into position and simultaneously the blower, Sanborn strip chart and Honeywell recorder strip chart were started. The dryer and recorder charts were allowed to run until no further noticeable change could be observed on the chart of the Sanborn recorder. The dryed sample was then quickly removed from the weighing frame and weighed to the nearest 0.01 pound. This weight was compared with the weight of the squeezed sample minus the weight change as indicated by the recorder.

It was necessary to leave the dryer in operation during the change of samples during the high temperature runs, since the transit time required for the temperature to stabilize approached the drying time.

CHAPTER VI

DISCUSSION OF RESULTS

All samples were dried under constant drying conditions; that is, they were exposed to air at constant temperature, humidity, and velocity. At high temperatures and velocities these conditions became more difficult to obtain, since the transit time required to reach constant drying conditions approached the drying time. The use of a dummy sample as explained in Chapter V minimized this problem, but it was impossible to obtain reliable data at temperatures above 260° F.

All samples were found to exhibit all four regions of the rate-of-drying curve. The critical moisture content of tufted wool carpet compared favorably with that listed by Bell and Grosberg (1) for 1/8 inch thick layers of knitted wool. The critical moisture content of nylons was found to be lower than that of wools. This was expected since the equilibrium moisture content given in Table 1 was much lower. A low surface temperature during drying in the unbound moisture region and then a sudden rise in temperature at the critical moisture content was observed in Figures 21 and 22 and was most noticeable in Figure 23 where a thermocouple was actually buried in the fibers. This was

also expected since the surface temperature during drying in the unbound region was approximately that of the wet bulb temperature.

The effect of variations in temperature, humidity, velocity, moisture content and results of analytical predictions will be discussed separately since each was an important portion of the investigation.

Effect of Air Humidity

Since the drying rate varies directly with the differance in humidity ratio between the drying substance and the air stream, increases in air humidity lowers the rates of drying. This could be observed most noticeably at lower temperatures, Figures 9 and 13, since the difference in humidity ratio was small. At higher temperatures the humidity ratio difference was so large that any small change in the inlet air humidity did not affect the rate-of-drying observably.

Effect of Air Velocity through the Sample

Neglecting conduction and radiation, the drying rate was increased directly by increases in velocity and exponentially by increases in the mass transfer coefficient.

The flow in the wind tunnel was found to be turbulent for data between 250 and 900 fpm, but the flow through the carpet was found to vary linearly with the pressure drop through the sample.

Although higher velocities create higher drying rates, there is a practical limit on the amount of air which can be forced through standard widths of carpet. Since the pressure drop varies linearly with the velocity, the difficulty of holding and supporting the material increases. For low velocities (up to 500 fpm) a standard tenter frame is sufficient to support the material. Slightly higher velocities can be reached using rollers below the tenter rail. For velocities above 800 fpm a perforated supporting chain belt must be used. In any event, a tenter frame is advantageous, since it stretches the shrunken carpet when it is wet, allowing higher velocities through the material. The allowable velocities, of course, depend on the weight of material being dried. The above limits were based on 32 oz./yd.^{2} material.

Effect of Air Temperature

Higher temperatures causing correspondingly higher humidity ratio differences had the effect of increasing the drying rate.

Effect of Moisture Content of Carpet

The amount of open-flow area was found to increase with decreasing moisture content. The cause of the smaller open area at high moisture contents was due in part to the presence of liquid water between the fibers and to the shrinkage of the wet material. This transit condition

caused a variation in the velocity flowing through the sample. This variation was most noticeable at high moisture contents which would be encountered in the initial adjustment period. During this adjustment, the liquid appeared to be forced from between the fibers by a mechanical process rather than being removed by diffusion. This phenomena can be noticed in Figures 18 and 20. After the moisture content has been reduced until drying was occurring in the unbound region, the variation in open-flow area was found to be slight, as indicated by constant drying rate. All analytical calculations were based on the open area in a dry sample.

The final drying rate or removal of internal moisture was found to be higher with synthetic fibers than with wools. This was due to the nonabsorbing nature of the fibers. Wool, cottons, and other hygroscopic materials tend to absorb and retain a definite percentage of moisture under definite conditions of air humidity. The synthetics are nonhygroscopic in nature; although, they do display a hygroscopic tendency but to a much lesser degree than wools or cottons. This can be observed in Table 1. For detailed information on the equilibrium moisture content, refer to Perry (12).

Critical Moisture Content

The analytically determination of the critical moisture content is still to be solved. None of the data in this investigation gave any indication to the method of

solution of this problem. According to Perry (12), the critical moisture content increases with an increase in the rate of drying and with an increase in the thickness of the layer being dried. According to Bell and Grosberg (1), the critical moisture contents are dependent on the amount of absorbed moisture, and to a much smaller extent, on the speed of drying and the structure of the material. Bell stated that they appear to be independent of the thickness of the material. In general, it can be said that the critical moisture content of an hygroscopic material is greater than a similar nonhygroscopic material of similar construction by the saturation amount of absorbed water. As can be seen, there is some disagreement on the variables which affect the critical moisture content. The analytical solution to this problem would allow the complete analytical determination of the drying time and, therefore, would be a great contribution to the field.

Correlation of Data by Dimensionless Numbers

The combined variables which were considered to affect the pressure drop of the air flowing through the carpet was correlated as explained in Chapter III, page 17. The correlation is shown in Table 15 and on Figure 8. It was found that data taken for all carpets tested correlated well using the parameters which were derived, although the parameters were not severely tested by the range of carpet samples tested.

Results of Analytical Predictions of the Drying Rates in Unbound Moisture Region

The analytical prediction of drying rates during the unbound moisture region was found to agree with experimental data to within 25 per cent. The accuracy was found to depend entirely on the dimensionless drag coefficient for high temperature runs and on the measurement of the dry and wet bulb temperature for low temperature runs. A comparison of analytical and experimental drying rates is presented in Table 16.

Results of Analytical Prediction of Drying Time During Falling Rate Period

The analytical prediction of the drying time during the falling rate period was found to agree with experimental data to within 35 per cent. The accuracy depended on the value of critical moisture content and constant drying rate. The sample was assumed dry when the moisture content had been reduced to 5 per cent of the critical moisture content. For hygroscopic fibers, this value was probably low. Since the equilibrium moisture content depends on the air humidity and to a lesser degree on the temperature, the equilibrium moisture content was not determined for each run.

CHAPTER VII

CONCLUSIONS

The time required to dry tufted carpet with through-flow drying is more than five times faster than any present method being used today. Drying rates and total drying time using the experimentally determined equilibrium moisture contents and drag coefficients can be predicted within 30 per cent.

The pressure differential across tufted carpet at a given temperature varies linearly with the flow rate through the material for velocities between 250 and 900 feet per minute. The open through-flow area increases with decreasing moisture content. The increase occurs most noticeably when the initial moisture content is above 200 per cent with little change occurring after reaching the unbound moisture region of drying.

CHAPTER VIII

RECOMMENDATIONS

Further Analysis of the Data

Efforts should be made to extend the analytical approach by Bell and Grosberg (1) to better fit small cylinders of fiber such as found in tufted carpet. An investigation of the critical moisture content and influencing variables would also be of great value. Along with such an analysis and the drying rates determined in this investigation, total drying time could be predicted analytically and compared with the drying time determined experimentally in this investigation.

Future Investigation

It is felt the following studies would merit consideration:

1. It would be of interest to determine the effect of the relative humidity of the air at temperatures above 250° F. on the drying rates. This would be of great commercial importance since it would give a direct indication of the amount of air which could be economically recirculated in industrial dryers. This investigation could be performed with the present wind tunnel dryer by injecting a water spray upstream to the finned tube section, Figure 1, and using a high temperature-humidity recorder controller up-

stream of the weighing section.

2. The analytical prediction of the pressure drop through tufted carpet would also be of interest. The result of such an analytical study could be compared with the experimental results plotted in Figure 8. Such a profitable study would add greatly to the eventual complete analytical prediction of drying rates. A related study was made by P. C. Carman (2) for the flow through granular beds. Lord (8) also investigated a similar problem for flow through woven fibers.

3. A study of the practicality of drying inlet air and its use in unheated air dryers would be of interest. This could be investigated by using an absorbing device through which the inlet air to the dryer could be directed. A silica jel absorber could be adapted to the present wind-tunnel dryer for this study. From an economical standpoint, this type of industrial drying merits consideration.

4. During the constant rate period (unbound moisture removal), if the heat necessary for vaporization is supplied only by conduction or convection through the same surface gas film through which the vapor diffuses, the surface temperature of the drying substance is the wet bulb temperature of the air (13). It would be interesting to see how the drying rate during this period could be increased when additional heat is supplied by radiation. The increased heat transfer should cause the surface temperature to be

higher than the wet-bulb temperature and, therefore, increase the rate of drying. See Ill. 4, page 544 (16). This forms a new expression for the temperature, humidity curve which has a steeper slope than the wet bulb curve.

5. Another interesting investigation would be the study of the effect of sound on the drying rate. It has been shown that sound has a definite effect on heat transfer. A similar effect should also occur in drying.

APPENDIX A

APPARATUS

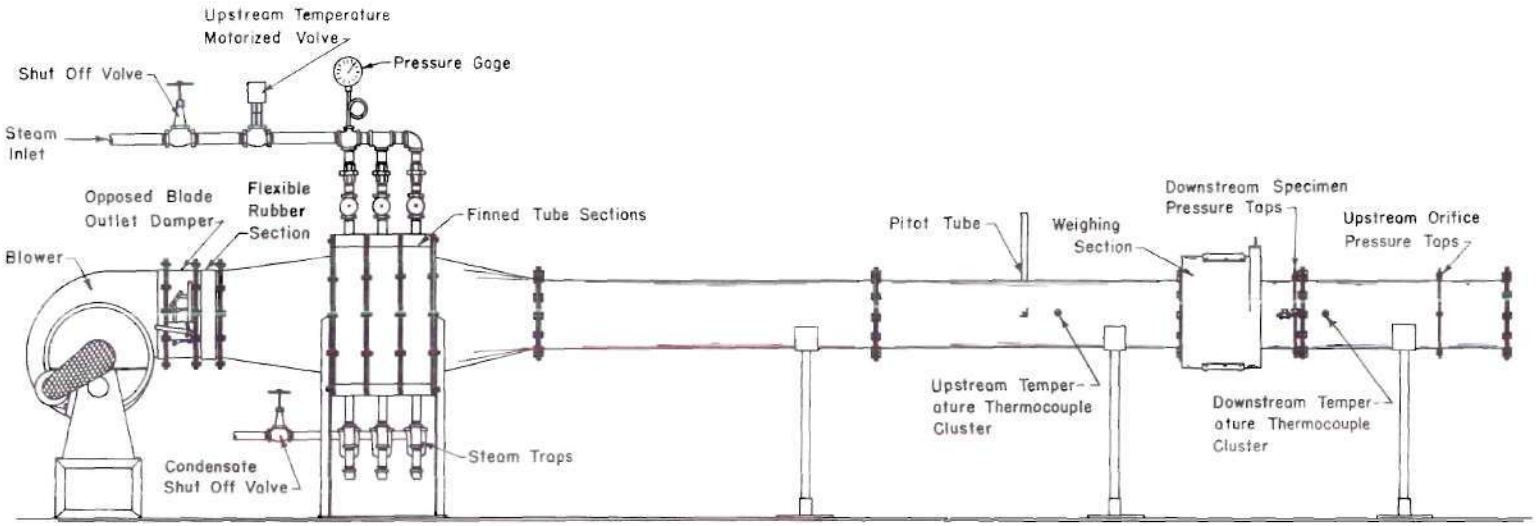

Figure 1. Schematic Diagram of Wind-Tunnel Dryer.

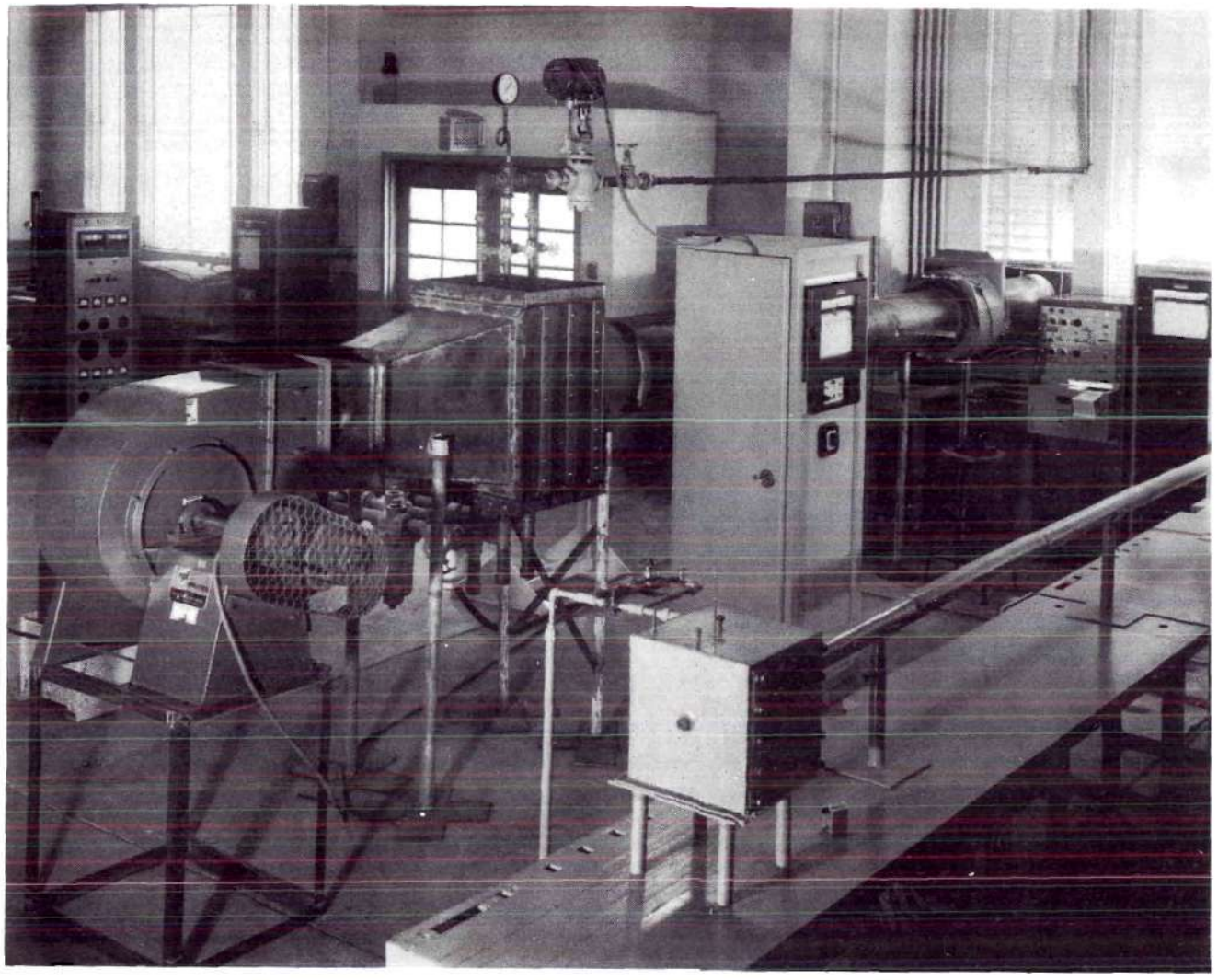

Figure 2. Photograph of Wind-Tunnel Dryer.

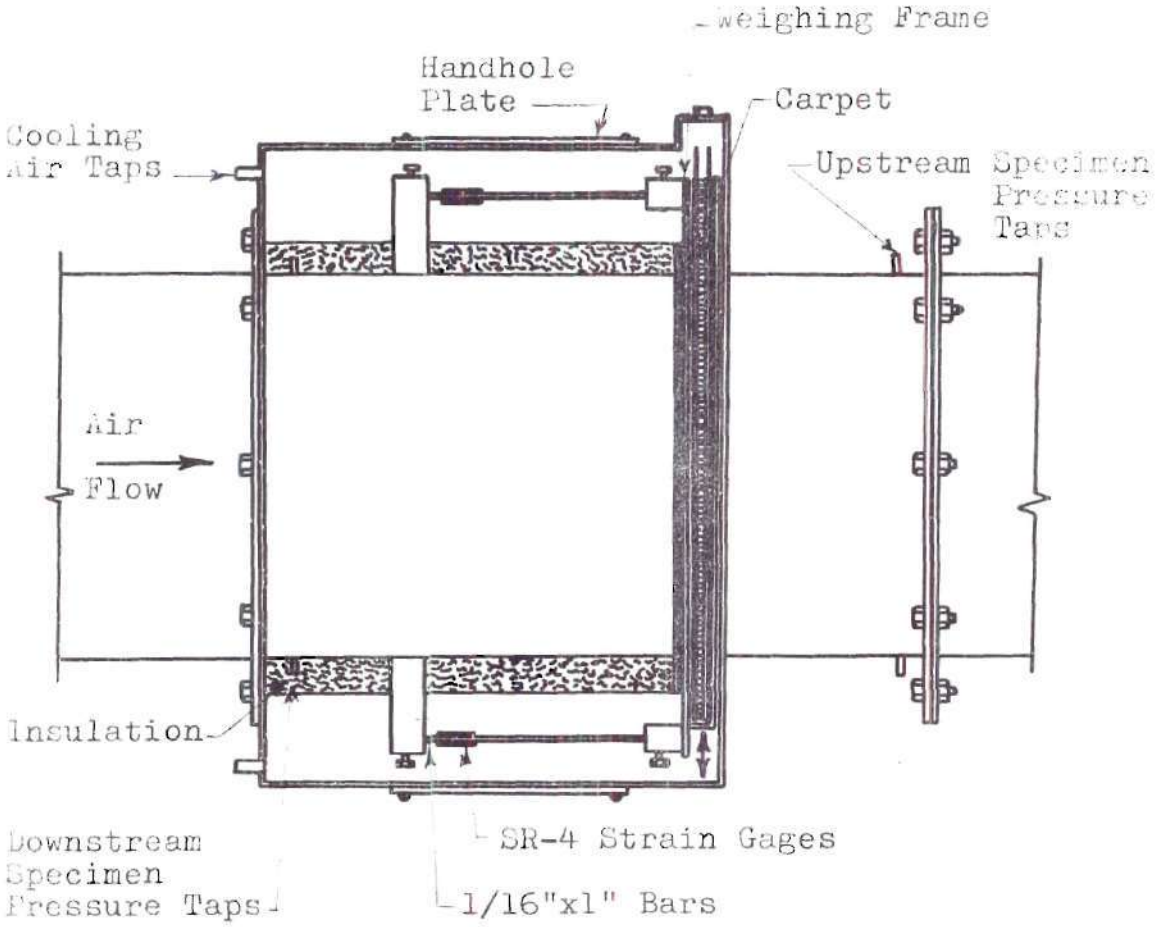

Figure 3. Schematic Diagram of Weighing Section

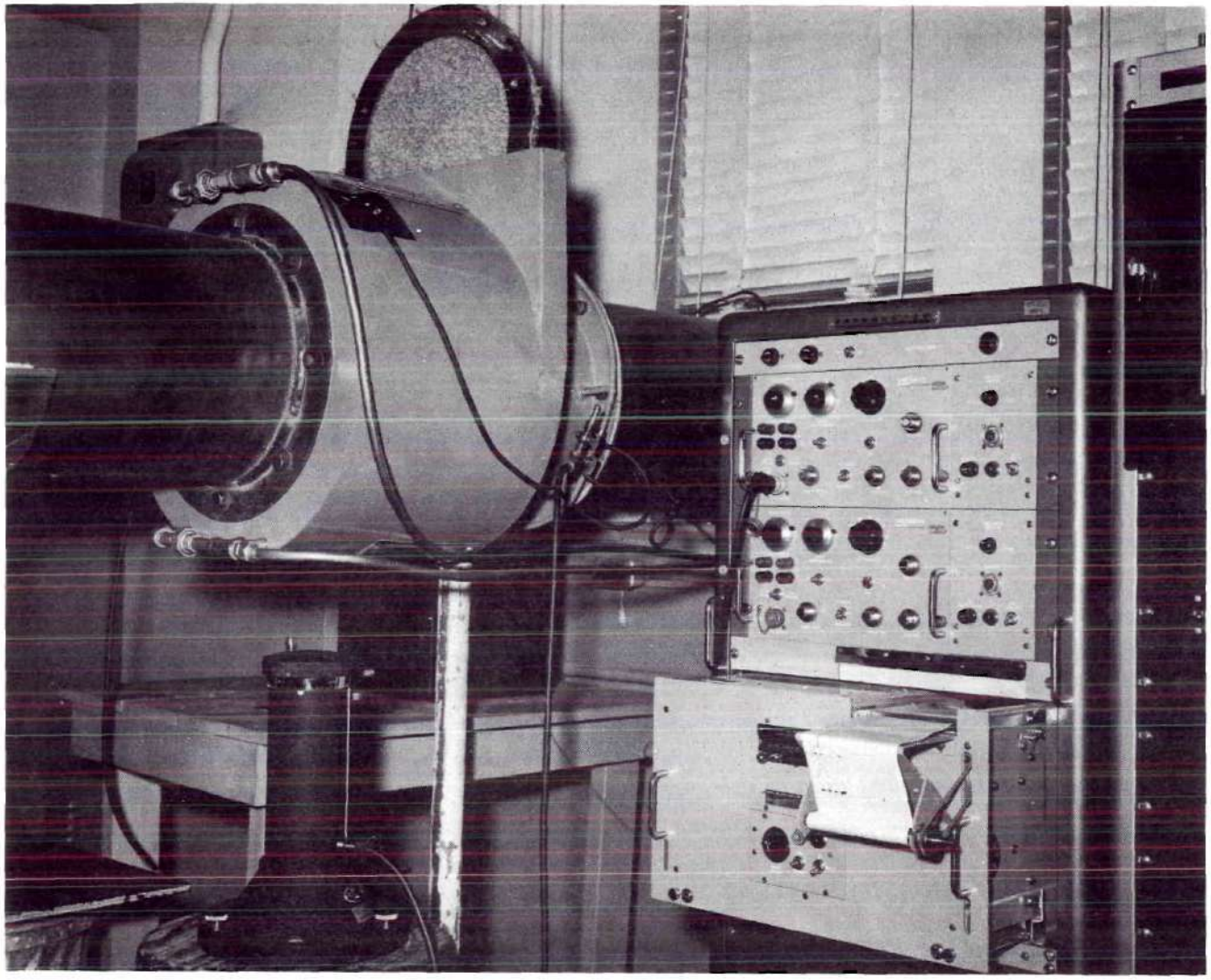

Figure 4. Photograph of Weighing Section and Sandborn Recorder.

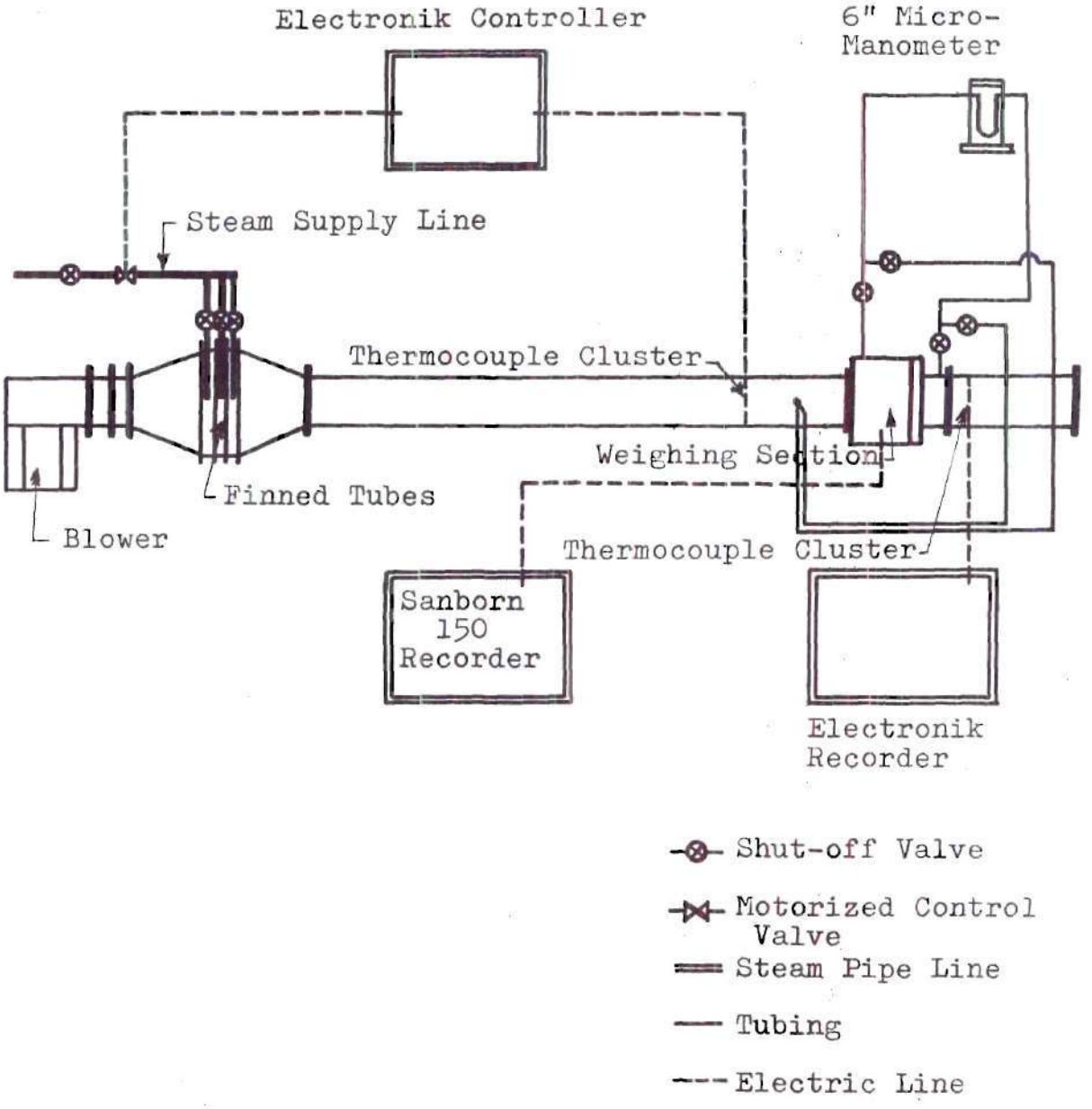

Figure 5. Schematic Diagram of Control, Measuring and Recording System

APPENDIX B

GRAPHICAL REPRESENTATION OF RESULTS

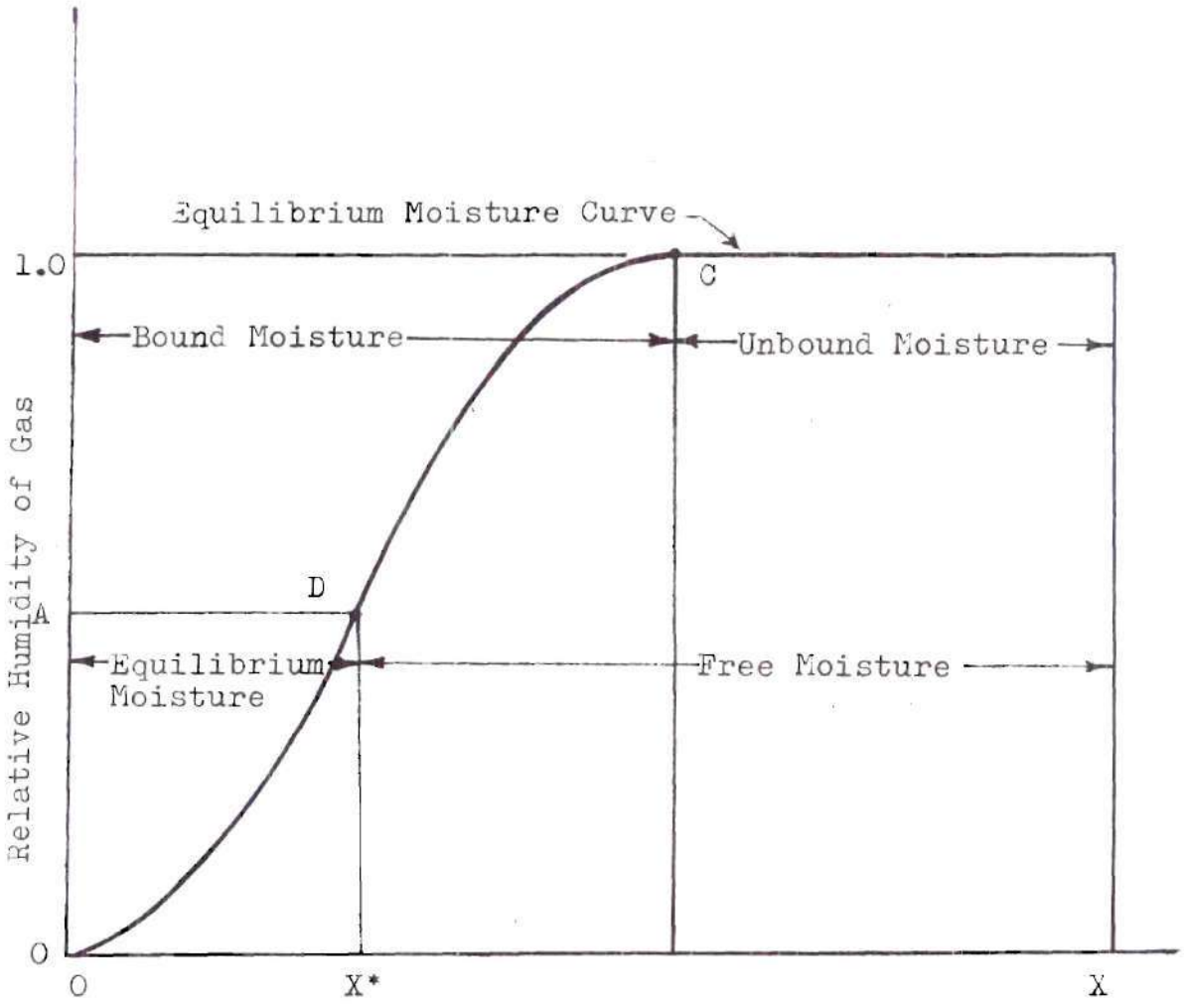

Figure 6. Types of Moisture

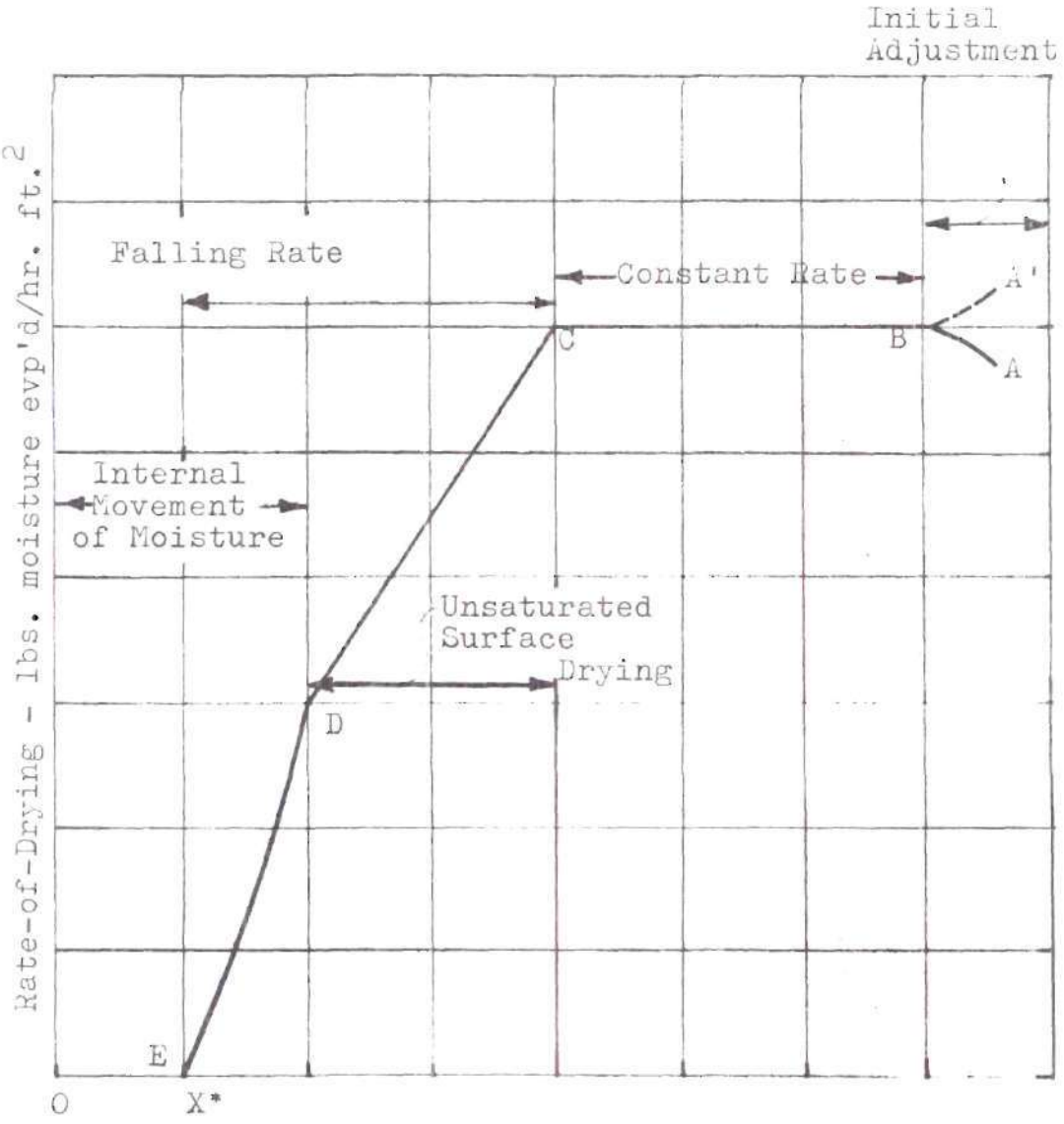

Figure 7. Typical Rate-of-Drying Curve

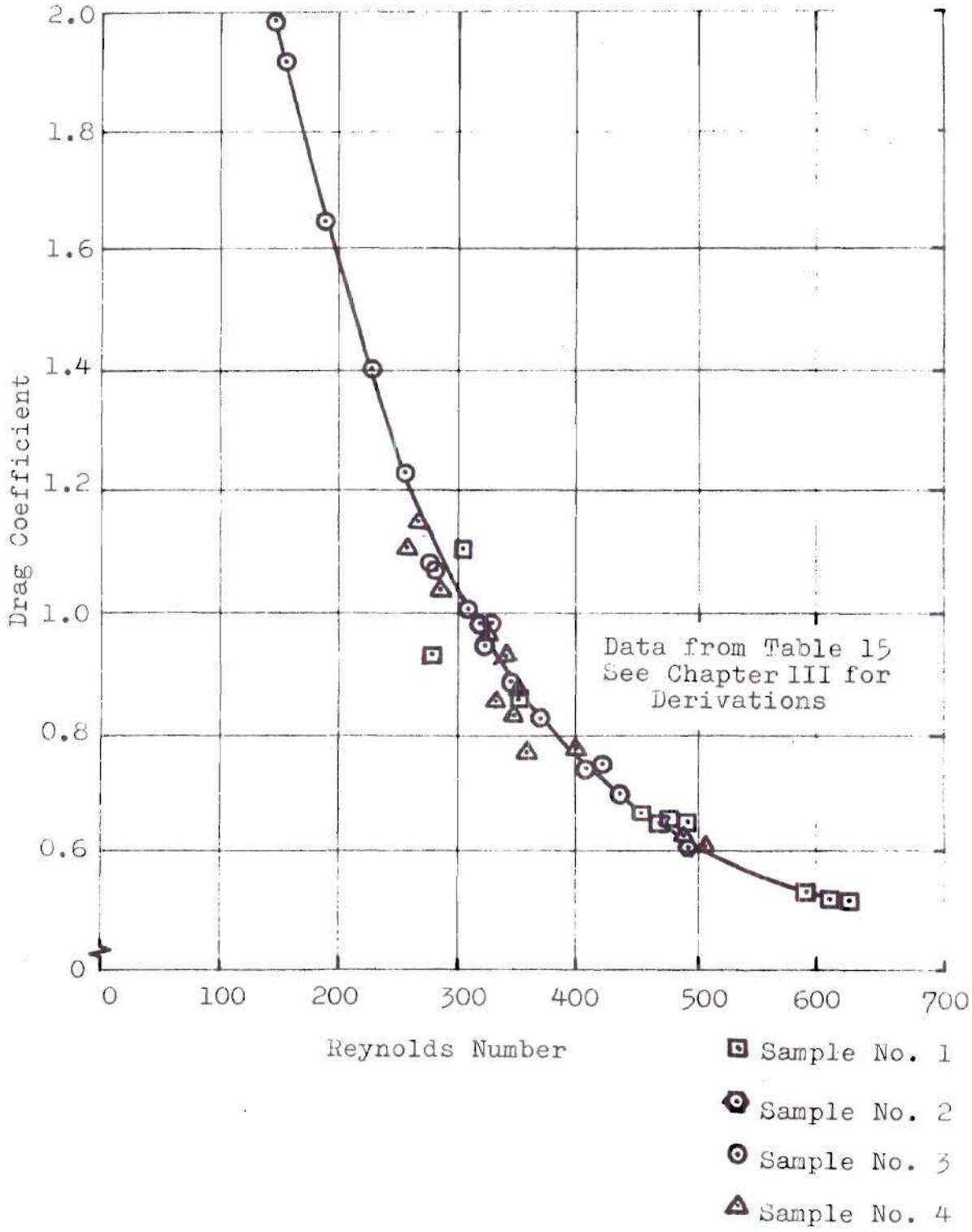

Figure 8. Dimensionless Parameter Correlation

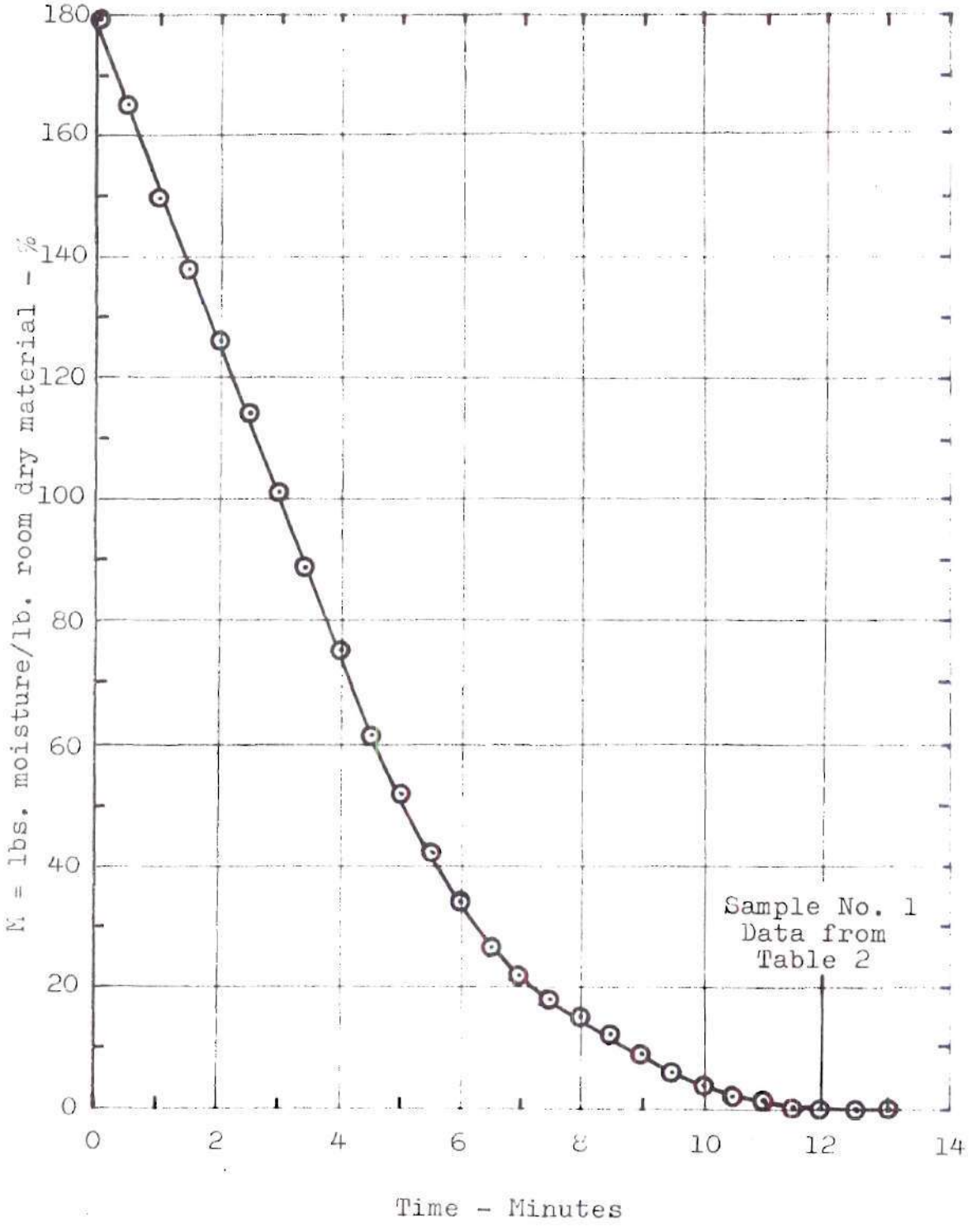

Figure 9. Drying Curve, Re = 625

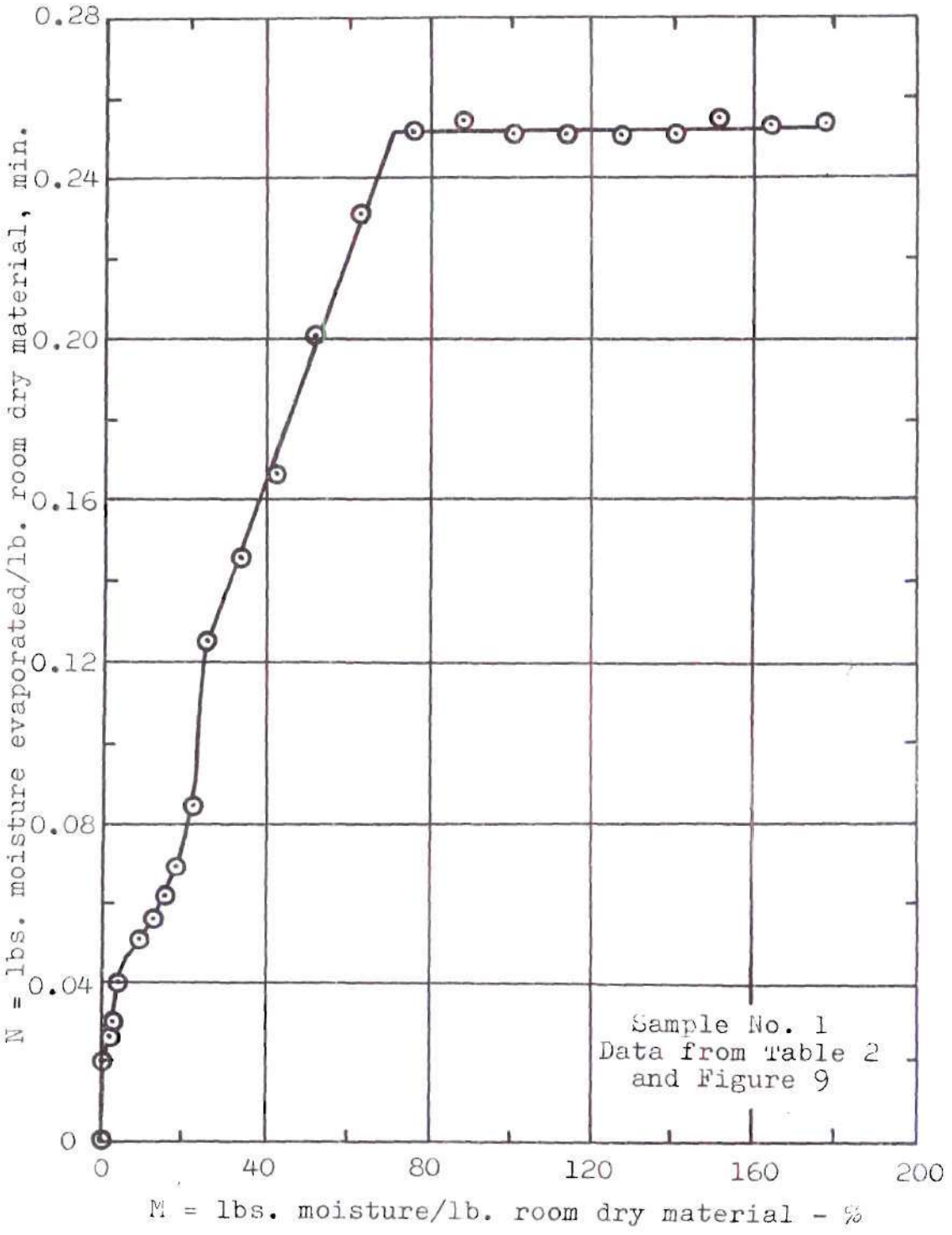

Figure 10. Rate-of-Drying Curve, Re = 625

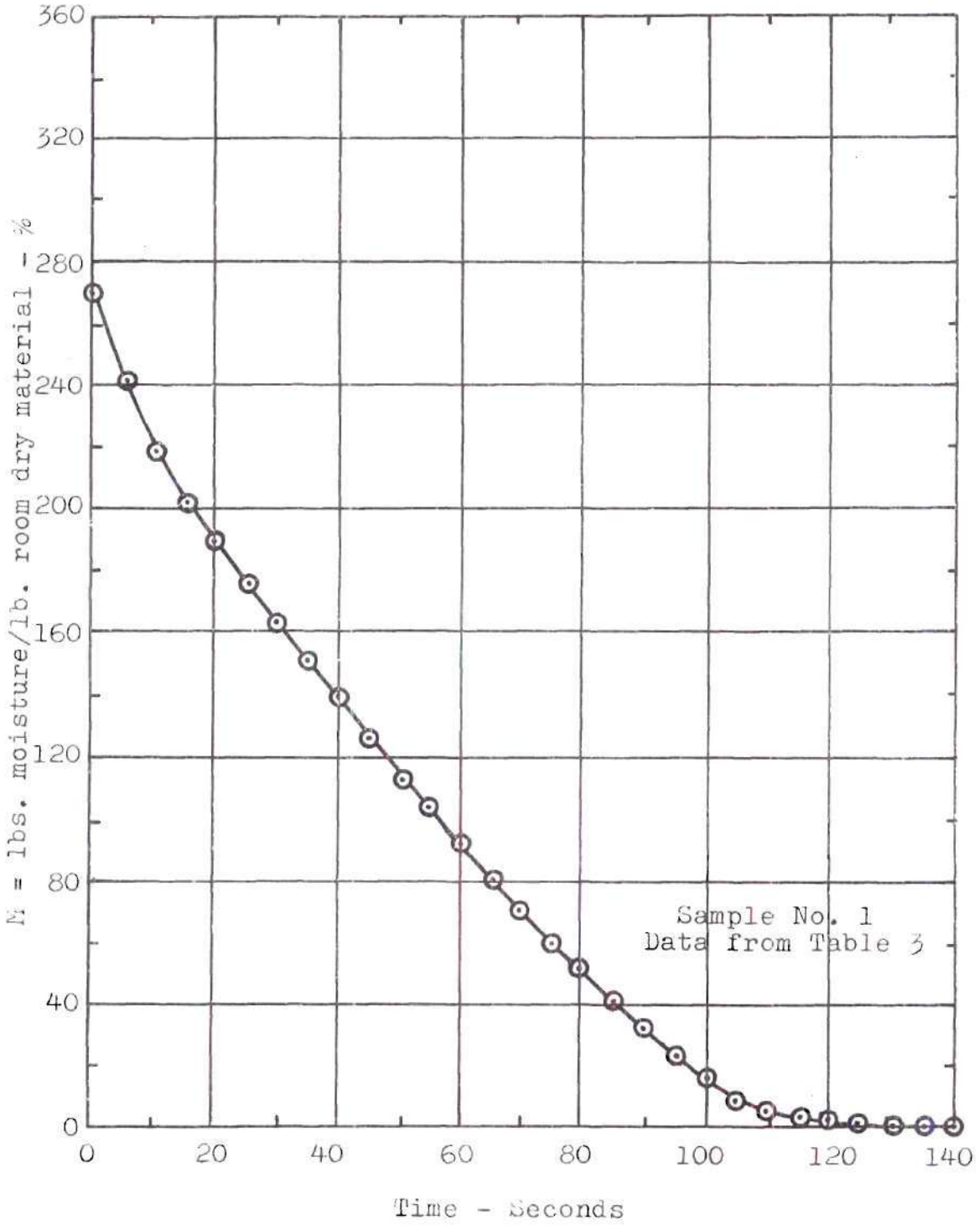

Figure 11. Drying Curve, Re = 274

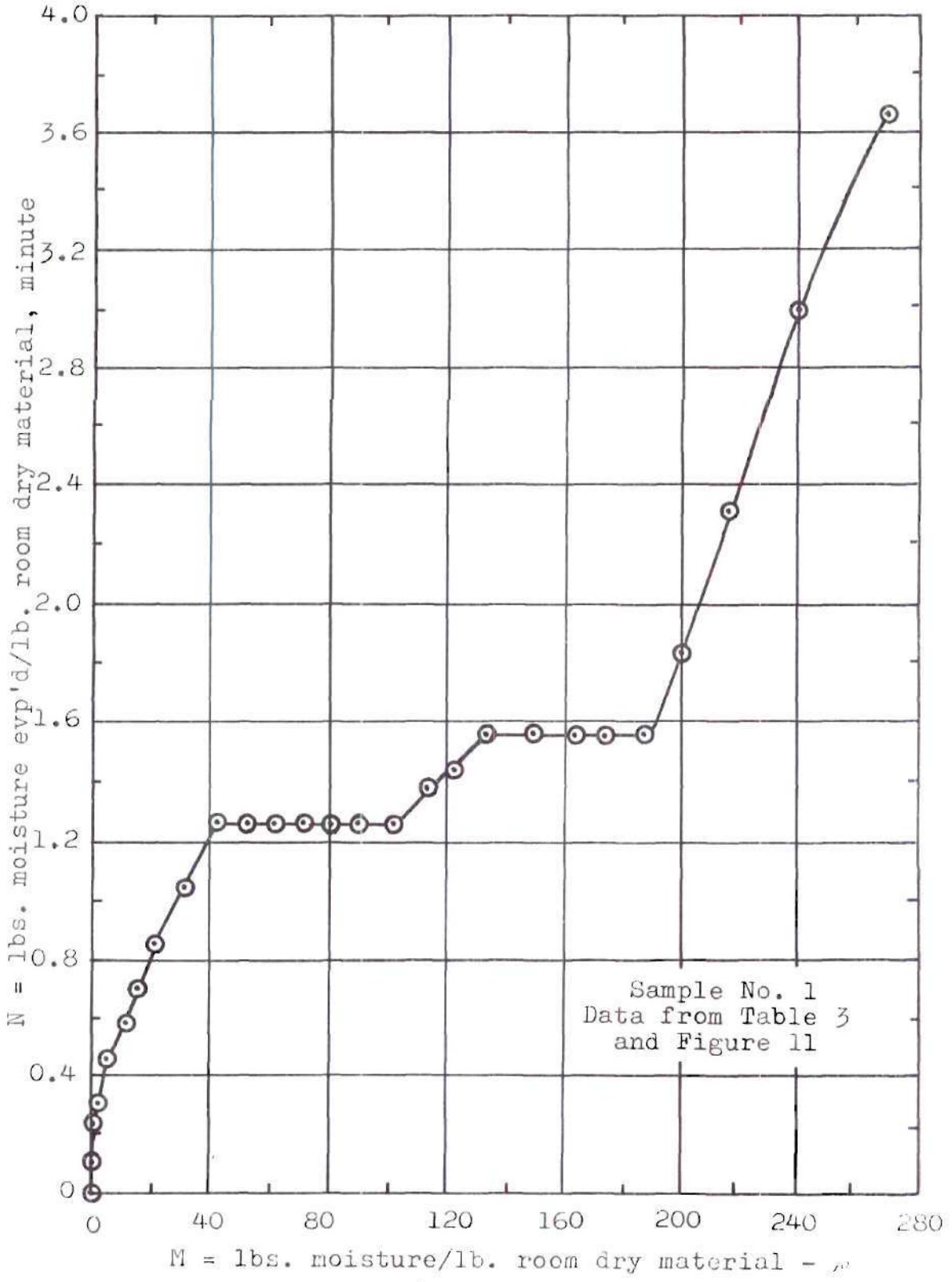

Figure 12. Rate-of-Drying Curve, Re = 274

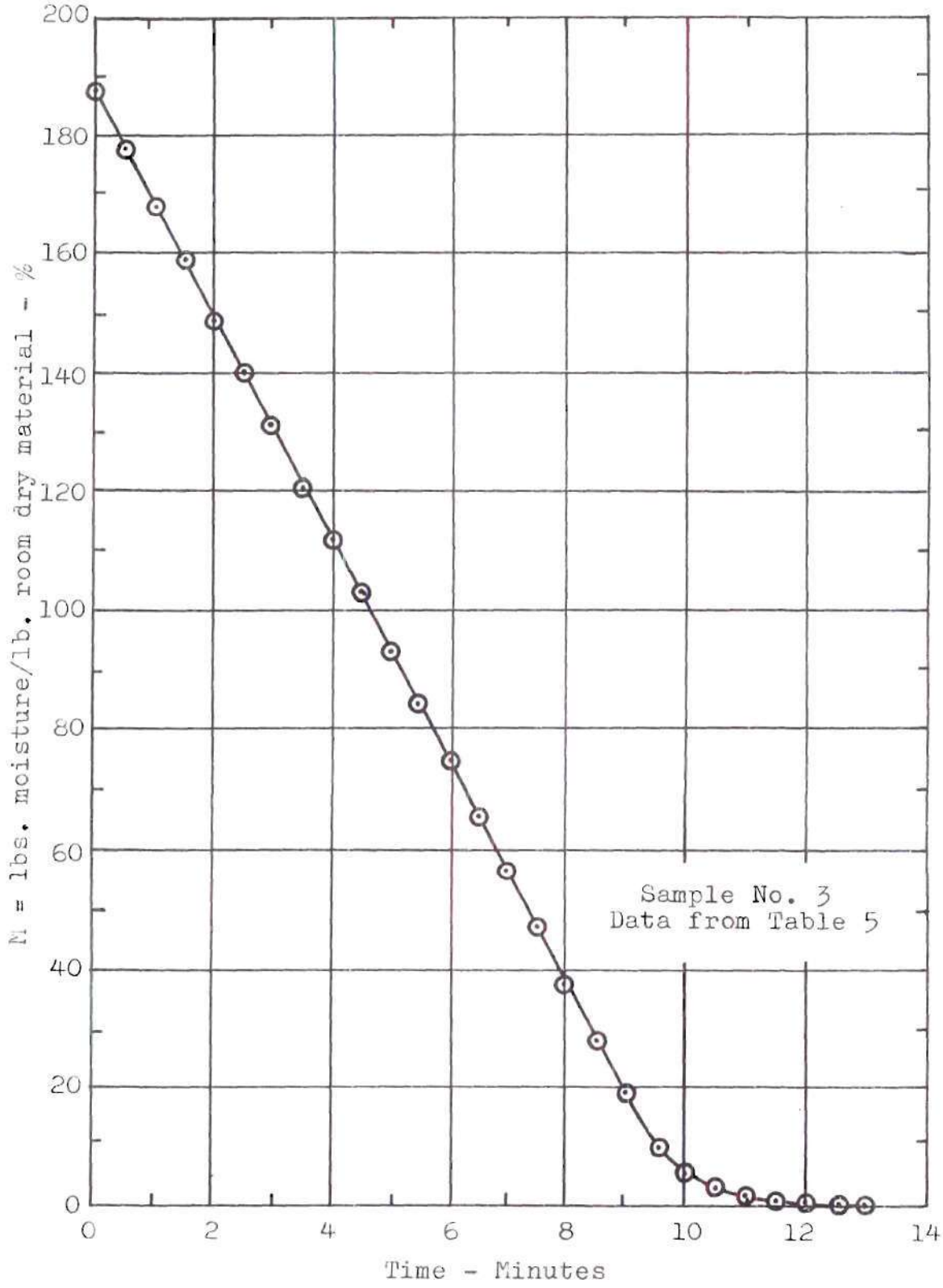

Figure 13. Drying Curve, Re = 420

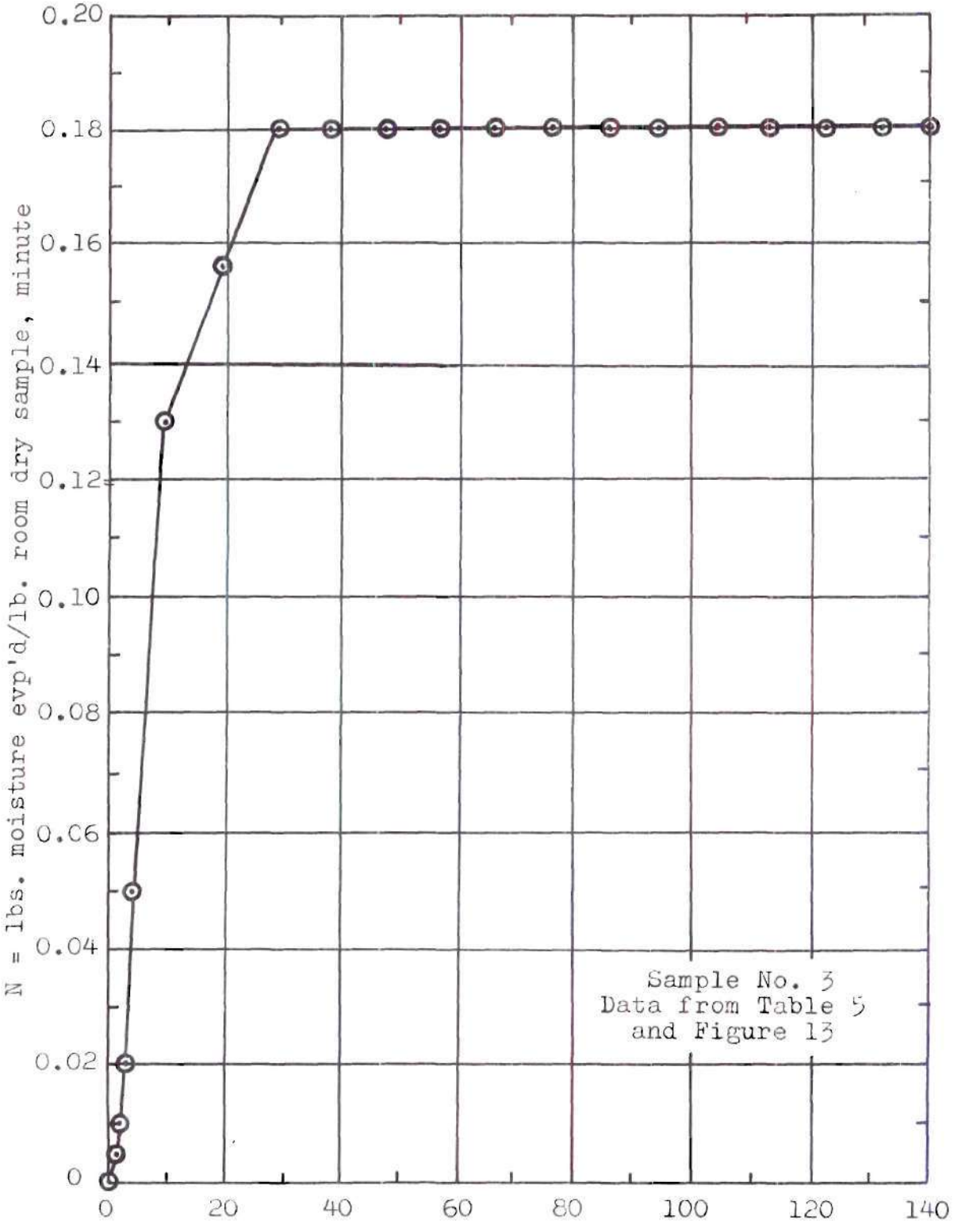

Figure 14. Rate-of-Drying Curve, Re = 420

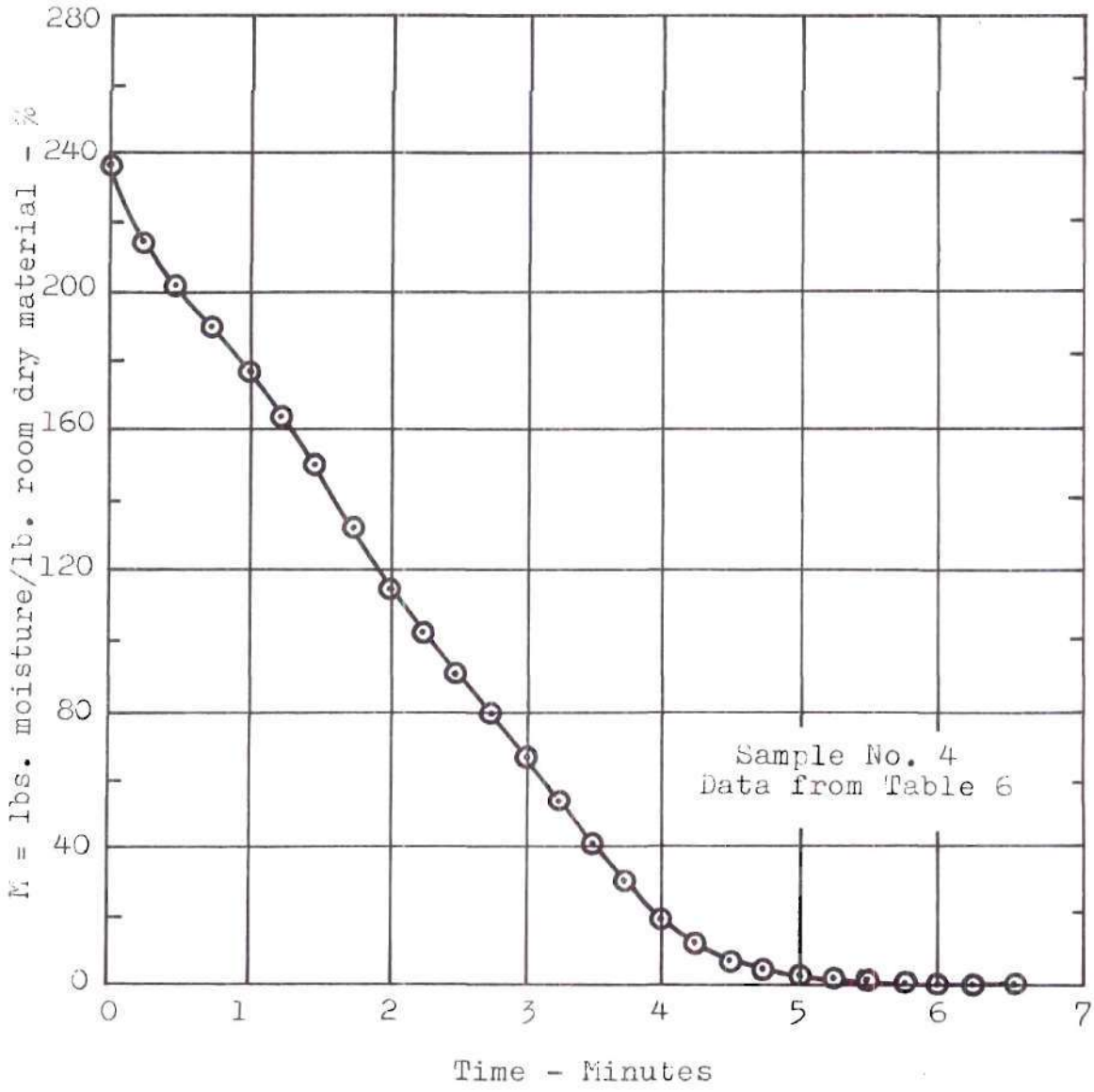

Figure 15. Drying Curve, Re = 285

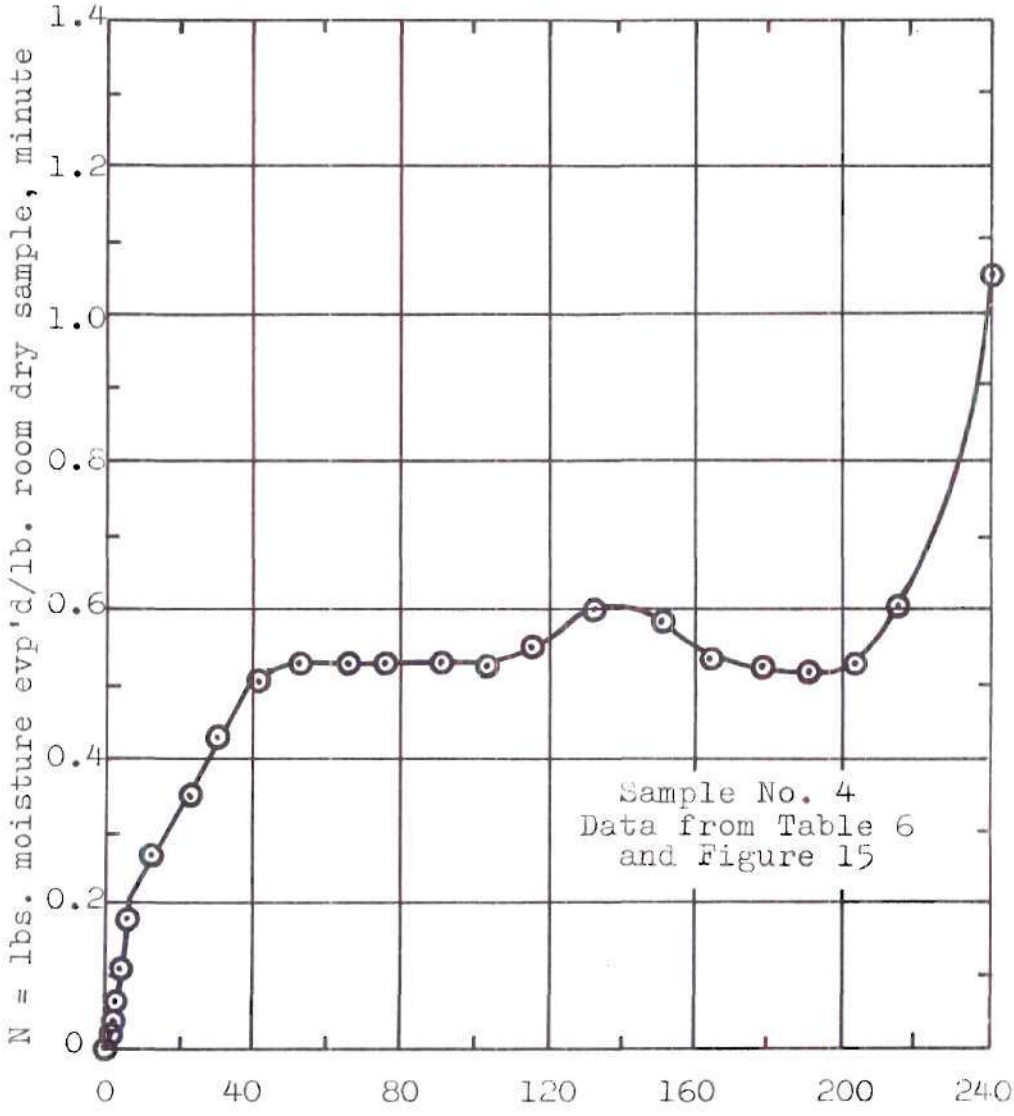

Figure 16. Rate-of-Drying Curve, Re = 285

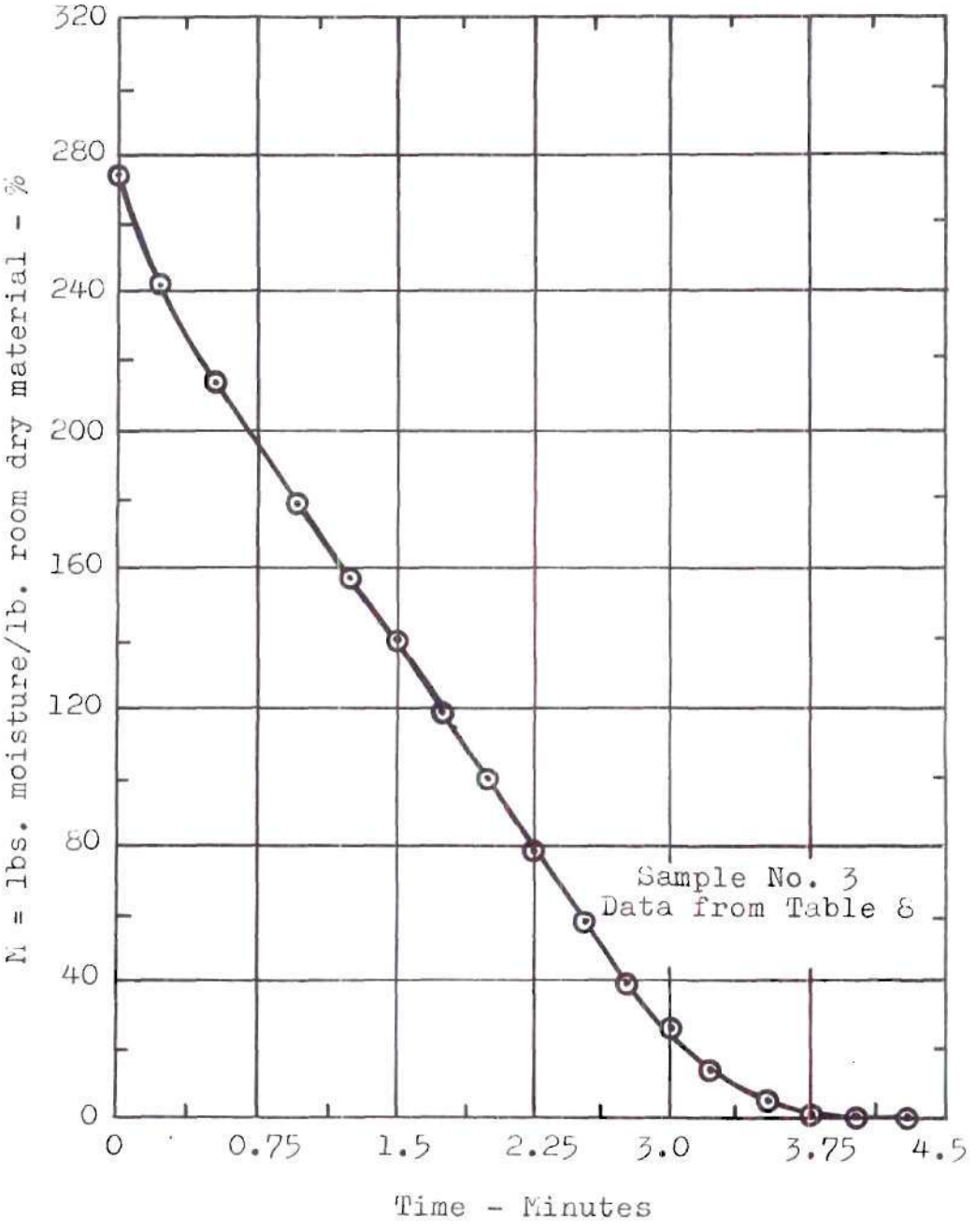

Figure 17. Drying Curve, Re = 517

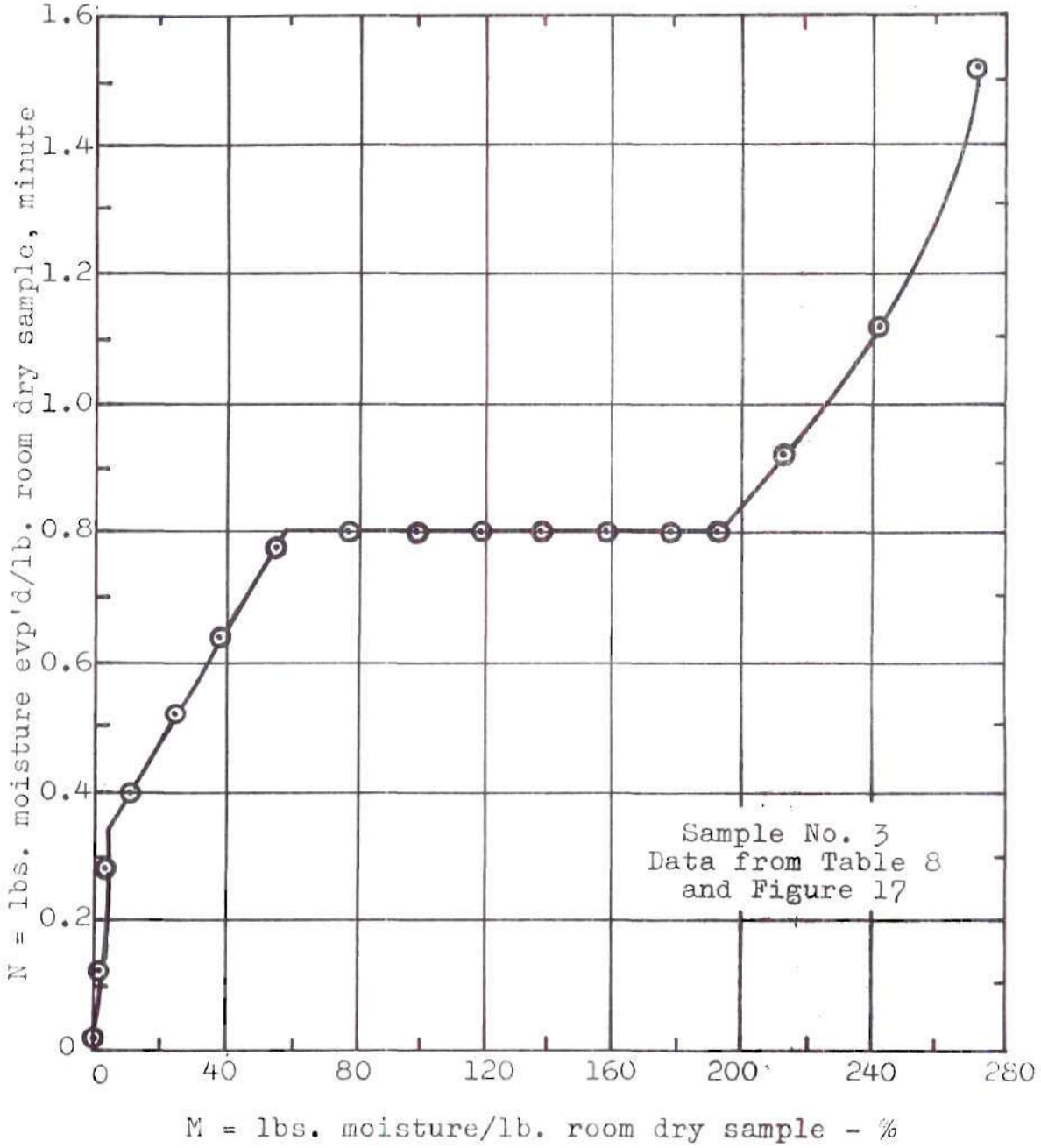

Figure 18. Rate-of-Drying Curve, Re = 317

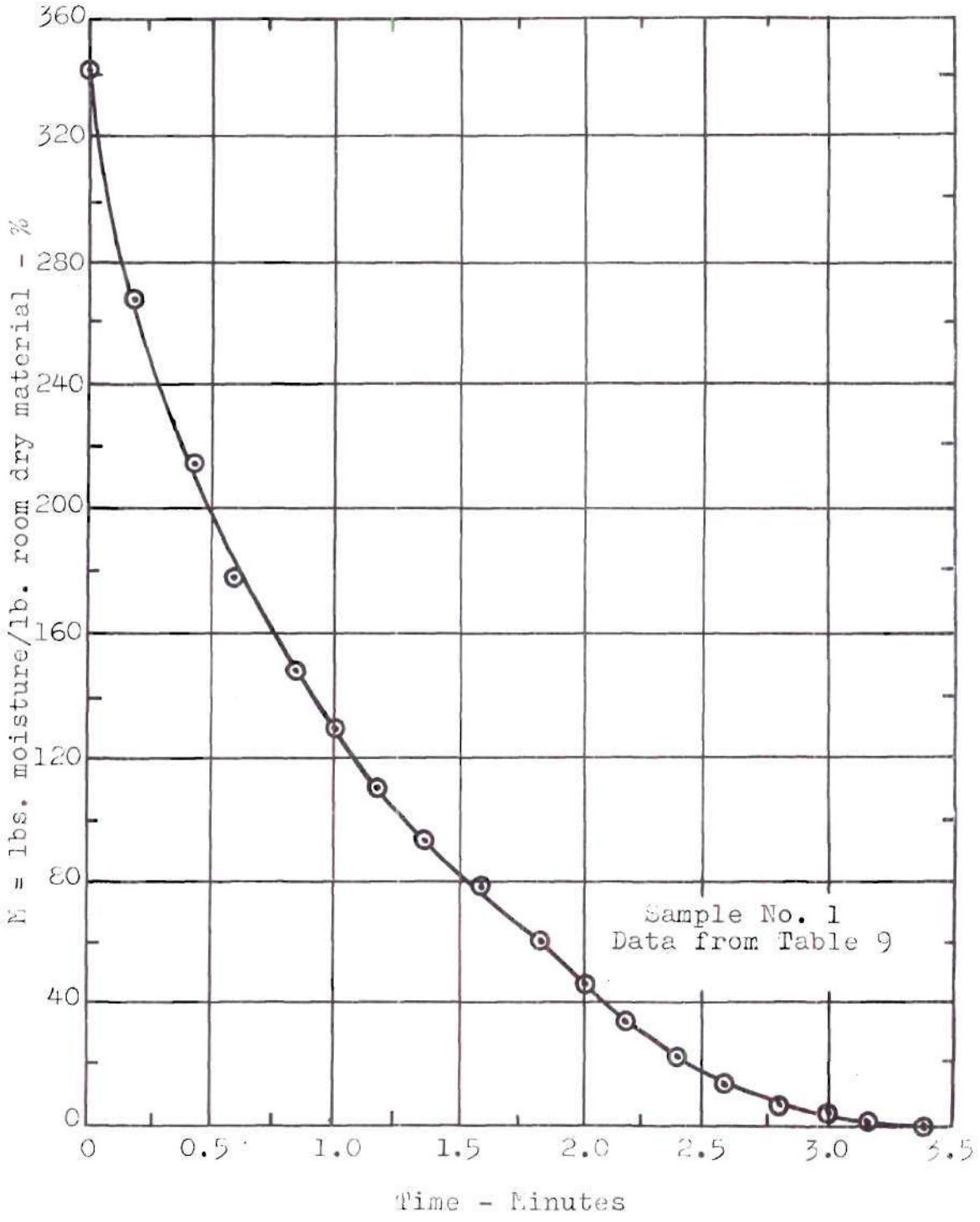

Figure 19. Drying Curve, Re = 356

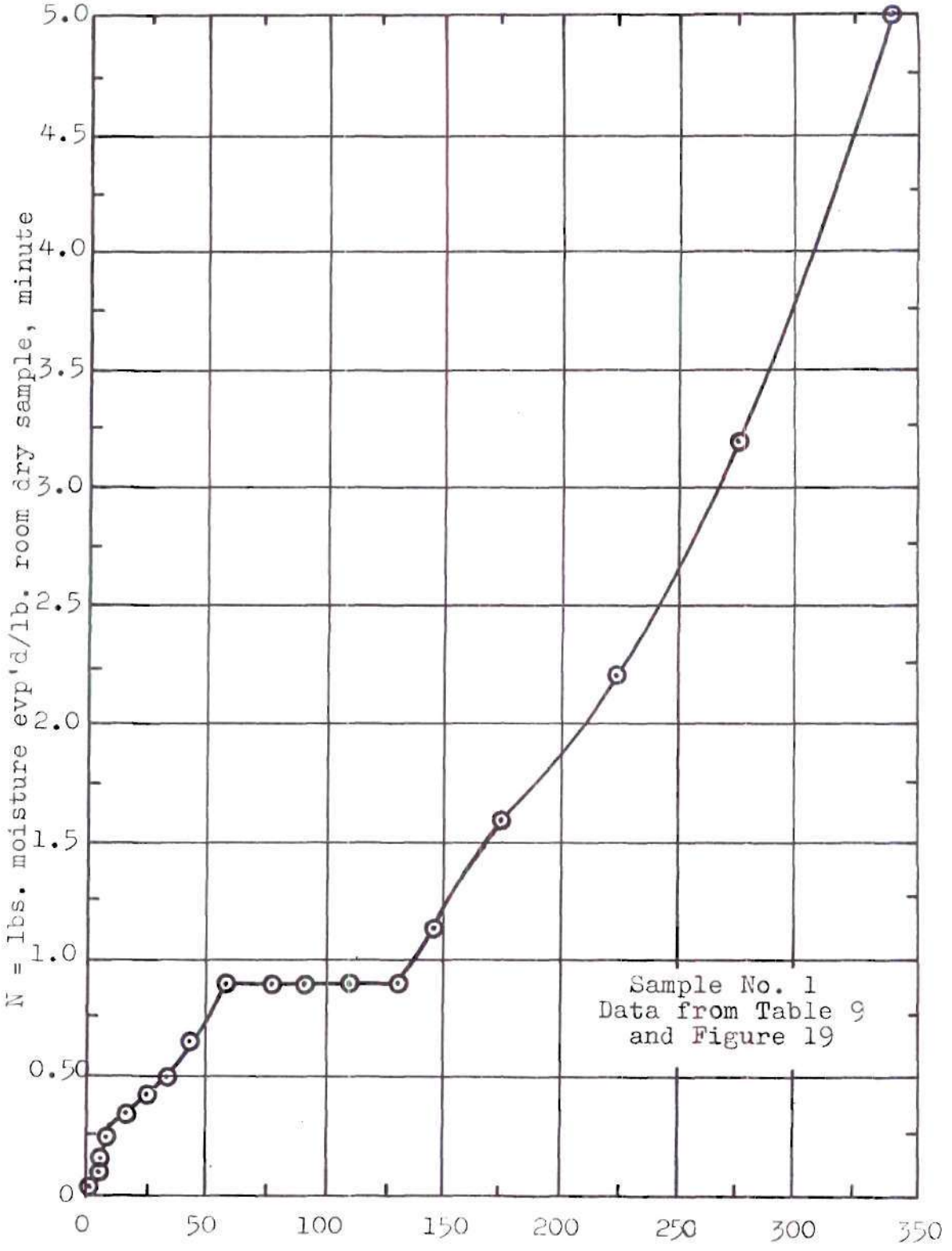

Figure 20. Rate-of-Drying Curve, Re = 356

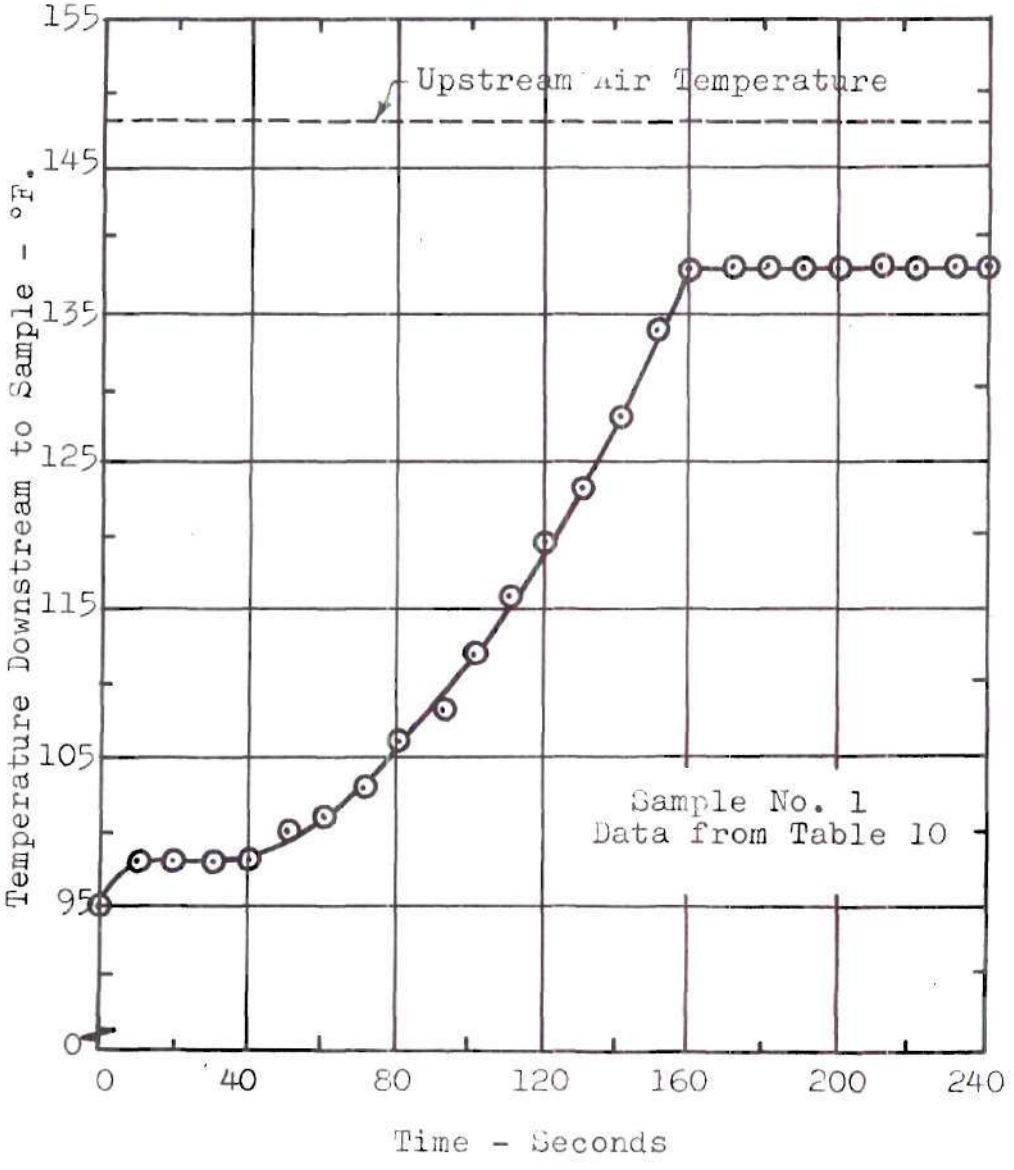

Figure 21. Temperature Downstream to Sample vs Time

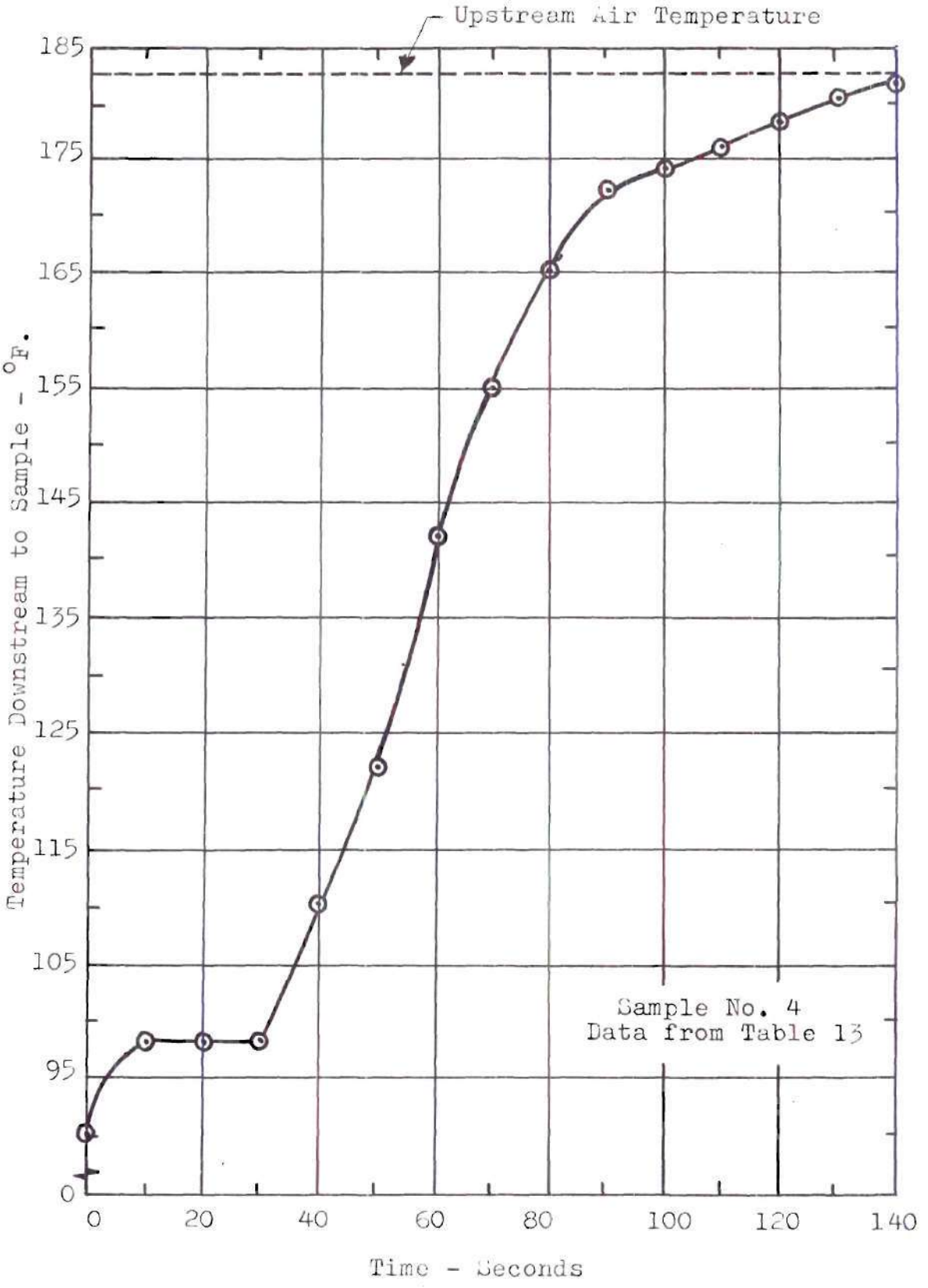

Figure 22. Temperature Downstream to Sample vs Time

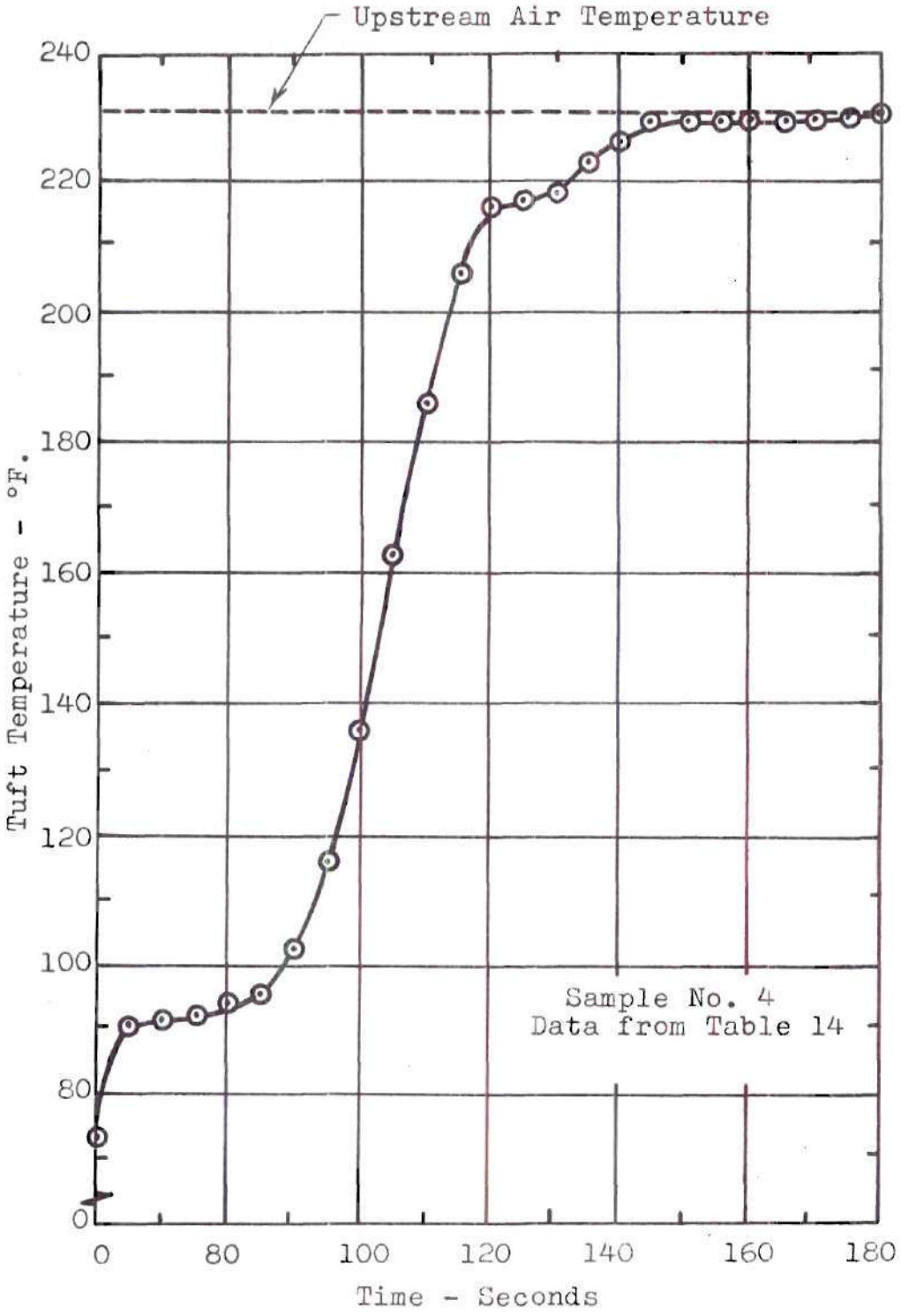

Figure 23. Tuft Temperature vs Time

APPENDIX C

CARPET DATA

Table 1. Carpet Sale

Sample	1	2	3	4
Fiber	Wool	Nylon (Tycora)	Nylon (Tycora)	Wool
Color	White/ Purple	Gold	Brown	Mixed
Sp. Gravity	1.32	1.14	1.14	1.32
Yarn Number*	2.4/3	one 5.1/3 with one 5.1/1	5.1/3	2.4/3
Backing	Jute	Jute	Jute	Jute
Wt. Backing, oz./yd.^{2}	9	9	9	10
Total Wt. oz./yd.^{2}	34	25	31	42
Yarn Dia.**	0.0247	0.0183	0.0183	0.0247
Equilibrium Moisture Content***				
70°F., 95% r.h.	21.9 @ 77F. 90% r.h.	8	8	21.9 @ 77F. 90% r.h.
70°F., 65% r.h.	16	4.2 to 4.5	4.2 to 4.5	16
Hgt. of Tuft	0.5	0.45	0.45	0.40

*Cotton yarn number is measured in terms of length of yarn per unit weight. No. 1 cotton has 840 yards per pound. No. 10 has 8,400 yards per pound. The count is inversely proportional to the size of the yarn.

**Yarn Diameter Conversion Table, Textile World, July, 1960, p. 60.

***Taken from Textile World, July, 1962, p. 158.

APPENDIX D

TYPICAL COMPUTATIONS

Experimental Data: Sample No. 1

Area of Sample = 113 in.^{2}
ΔP (Sample) = 2.4140 in. H_2O
m = 34 oz./yd.^{2}
W_b = 9 oz./yd.^{2}
S.G. = 1.32
a = 15
b = 13
n = 6.25
T_d = 60°F.
T_w = 57°F.
T_l = 262°F.
V = 694 fpm

Pressure Drop Calculation

The yard number of the backing is

$$N = \frac{a+b}{W_b} = \frac{(13+15)(36)(16)}{9(840)} = 2.11$$

The respective fiber diameter is

$$d_f = \frac{0.0438}{\left[2.11(1.32)\right]^{1/2}} = 0.0263 \text{ in.}$$

From equation (2)

$$A_f = (a+b+n)d_f = (13+15+6.25)(0.0263) = 0.904 \text{ in.}^2/\text{in.}^2$$

The open area is

$$A_o = A - A_f = 1.00 - 0.904 = 0.096 \text{ in.}^2/\text{in.}^2 = 0.0755 \text{ ft.}^2/\text{sample}$$

The number of openings is

$$N_o = a(b-n) = 15(13-6.25)(113) = 11,420 \text{ openings/sample}$$

The hydraulic diameter is

$$d_h = \frac{1}{4}\sqrt{\frac{A_o}{N_o}} = \frac{1}{4}\sqrt{\frac{0.0755}{11,420}} = 0.000642 \text{ ft.}$$

From Handbook of Air Conditioning Heating and Ventilating for $T_d = 60°F.$ and $T_w = 57°F.$, the relative humidity is 83.6 per cent. The saturated water vapor pressure at 60°F. is 0.2563 psia; therefore,

$$P_v = 0.836\ (0.2563) = 0.2140 \text{ psia}$$

It follows that

$$P_a = 14.710 - 0.2140 = 14.496 \text{ psia}$$

The density of the air-water vapor mixture is

$$\rho_m = \frac{P_a + 0.622P_v}{R_a T_1} = \frac{\left[14.496+0.622(0.214)\right](144)}{53.35(722)} = 0.0549 \text{ lb./ft.}^3$$

From Table A - 3, Kreith (6)

$$\mu = 1.545 \times 10^{-5} \text{ lbm/ft. - sec.}$$

From equation (1), the Reynolds number is

$$Re = \frac{Qd_h \rho_m}{A_o \mu} = \frac{545(0.000642)(0.0549)}{0.0755(1.545\times10^{-5})(60)} = 274 \qquad \text{Ans.}$$

From equation (12), the drag coefficient is

$$C_f = \frac{2g_c \Delta P A_o^2}{\rho_m Q^2} = \frac{(2)(32.2)(2.414)(5.204)(0.0755)^2(3600)}{0.0549(545)^2}$$

$$= 0.916 \qquad \text{Ans.}$$

Constant Rate Period Calculation

From Psychrometric Chart ω_1 = 64.5 grains/lbm air

ω_s =328.0 grains/lbm air

The maximum rate of water removal is

$$\left(\frac{dm_w}{dt}\right)_{max} = \rho_m V A_o (\omega_s - \omega_1) = 0.0549(545)\left(\frac{328.0-64.5}{7000}\right)$$

$$= 1.13 \frac{\text{lbm } H_2O}{\text{min}}$$

and

$$\left(\frac{dM}{dt}\right)_{max} = \frac{1.13}{0.33} = 3.43 \frac{\text{lbm } H_2O}{\text{lbm room dry sample, min.}}$$

From equation (27), the rate of water removal is

$$\frac{dM}{dt} = \left(\frac{dM}{dt}\right)_{max}\left[1-e^{-\frac{C_f}{2}\left(\frac{D_{\zeta}\rho_m}{\mu}\right)^{2/3}}\right]$$

$$\frac{C_f}{2}\left(\frac{D_{\zeta}\rho_m}{\mu}\right)^{2/3} = \frac{0.916}{2}(1.54)^{2/3} = 0.612$$

$$\frac{dM}{dt} = 3.43\left(1-e^{0.612}\right) = 1.750 \frac{\text{lbm } H_2O}{\text{lbm room dry sample, min.}} \text{ Ans.}$$

Falling Rate Period Calculation

From Table 3, $M_c = 55\%$

The drying time from equation (34) is

$$t - t_c = 2.9957 \frac{M_c}{(dM/dt)_{max}} = 2.9957 \frac{0.55}{(1.75)} = 0.943 \text{ min.} \quad \text{Ans.}$$

APPENDIX E

TABULATED TEST DATA

Table 2. Data for Drying of Sample No. 1

Air Data: Tunnel Temperature, dry - 72°F.
Room Temperature, dry - 74°F.
Room Temperature, wet - 56°F.
Velocity, dry sample - 815 fpm

Sample Data: Sample No. 1 - See Table 1
Pressure drop through sample, dry-2.2828 in.H_2O
Pressure drop through sample, wet-2.2285 in.H_2O

Time (min.)	Moisture Content* (lbs. moisture/lb. dry sample)	Drying Rate (lbs. moisture/lb. dry sample, min.)
0	1.79	0.254
0.5	1.64	0.254
1.0	1.50	0.256
1.5	1.37	0.250
2.0	1.25	0.250
2.5	1.14	0.250
3.0	1.00	0.250
3.5	0.88	0.260
4.0	0.76	0.250
4.5	0.61	0.230
5.0	0.52	0.200
5.5	0.42	0.167
6.0	0.34	0.148
6.5	0.26	0.125
7.0	0.22	0.084
7.5	0.18	0.071
8.0	0.15	0.061
8.5	0.12	0.058
9.0	0.09	0.053
9.5	0.06	0.040
10.0	0.04	0.030
10.5	0.03	0.028
11.0	0.02	0.021
11.5	0.01	0.01
12.0	0	0

*Moisture Content is based on the weight of the sample at its equilibrium moisture content corresponding to room conditions listed above.

Table 3. Data for Drying of Sample No. 1

Air Data: Tunnel Temperature - 262°F.
Room Temperature, dry - 60°F.
Room Temperature, wet - 57°F.
Velocity, dry sample - 694 fpm

Sample Data: Sample No. 1 - See Table 1
Pressure drop through dry sample-2.4140 in.H_2O

Time (sec.)	Moisture Content %	Drying Rate (lbs. water evp'd/ lb. sample, min.)
0	270	3.66
5	240	2.94
10	217	2.31
15	202	1.83
20	188	1.56
25	176	1.56
30	162	1.56
35	150	1.56
40	135	1.56
45	124	1.44
50	113	1.38
55	102	1.26
60	91.5	1.26
65	81.0	1.26
70	72.5	1.26
75	62.0	1.26
80	52.8	1.26
85	43.0	1.26
90	32.3	1.14
95	21.5	0.84
100	16.1	0.69
105	10.8	0.58
110	5.4	0.45
115	2.7	0.30
120	1.0	0.24
125	0	0.12
130	0	0.06

Table 4. Data for Drying of Sample No. 2

Air Data:	Tunnel Temperature	- 72°F.
	Room Temperature, dry	- 72°F.
	Room Temperature, wet	- 62°F.
	Velocity, dry sample	- 747 fpm
Sample Data:	Sample No. 2 - See Table 1	
	Pressure drop through sample, wet-2.4425 in.H_2O	
	Pressure drop through sample, dry-2.3140 in.H_2O	

Time (min.)	Moisture Content (lbs. moisture/lb. room dry sample)	Drying Rate (lbs. moisture evp'd/lb. room dry sample, minute)
0	295	0.90
0.33	261	0.90
0.66	236	0.90
1.00	206	0.90
1.33	185	0.74
1.66	155	0.60
2.00	135	0.53
2.33	120	0.49
2.66	108	0.46
3.00	90	0.40
3.33	76	0.32
3.66	65.2	0.28
4.00	57.6	0.24
4.33	50.1	0.20
4.66	42.5	0.18
5.00	37.5	0.17
5.33	32.5	0.17
5.66	26.0	0.17
6.00	20.0	0.16
6.33	15.0	0.15
6.66	10.0	0.13
7.00	7.5	0.10
7.33	5.0	0.08
7.66	2.5	0.07
8.00	0	0.05
8.33	0	0
8.66	0	0

Table 5. Data for Drying of Sample No. 3

Air Data: Tunnel Temperature, dry - 73°F.
Room Temperature, dry - 73°F.
Room Temperature, wet - 64°F.
Velocity, dry sample -655 fpm

Sample Data: Sample No. 3 - See Table 1
Pressure drop through sample, wet-2.445 in. H_2O
Pressure drop through sample, dry-2.375 in. H_2O

Time (min.)	Moisture Content (lbs. moisture/lb. room dry sample)	Drying Rate (lbs. moisture/ lb. room dry sample, min.)
0	187	0.18
0.5	177	0.18
1.0	168	0.18
1.5	159	0.18
2.0	149	0.18
2.5	140	0.18
3.0	131	0.18
3.5	121	0.18
4.0	112	0.18
4.5	103	0.18
5.0	93.5	0.18
5.5	84.2	0.18
6.0	74.8	0.18
6.5	65.5	0.18
7.0	56.0	0.18
7.5	46.7	0.18
8.0	37.4	0.18
8.5	28.0	0.18
9.0	18.7	0.155
9.5	9.35	0.130
10.0	4.68	0.08
10.5	3.74	0.05
11.0	2.34	0.02
11.5	1.40	0.01
12.0	0	0.005
12.5	0	0
13.0	0	0

Table 6. Data for Drying of Sample No. 4

Air Data: Tunnel Temperature, dry - 230°F.
Room Temperature, dry - 72°F.
Room Temperature, wet - 63°F.
Velocity, dry sample - 640 fpm

Sample Data: Sample No. 4 - See Table 1
Pressure drop through sample, dry-2.4855 in.H_2O
Pressure drop through sample, wet-2.2650 in.H_2O

Time (min.)	Moisture Content (lbs. moisture/lb. room dry sample %)	Drying Rate (lbs. moisture/ lb. room dry sample, min.)
0	239	1.04
0.25	214	0.60
0.50	202	0.52
0.75	190	0.51
1.00	177	0.52
1.25	163	0.53
1.50	151	0.58
1.75	133	0.60
2.00	115	0.54
2.25	102	0.52
2.50	90	0.52
2.75	77.7	0.52
3.00	65.4	0.52
3.25	52.9	0.52
3.50	40.5	0.50
3.75	31.1	0.42
4.00	21.8	0.34
4.25	12.4	0.26
4.50	6.21	0.17
4.75	4.65	0.10
5.00	3.11	0.06
5.25	1.55	0.03
5.50	0	0.02
5.75	0	0.01
6.00	0	0
6.25	0	0

Table 7. Data for Drying of Sample No. 4

Air Data:	Tunnel Temperature, dry - 73°F. Room Temperature, dry - 72°F. Room Temperature, wet - 63°F. Velocity, dry sample - 720 fpm
Sample Data:	Sample No. 4 - See Table 1 Pressure drop through sample, dry-2.400 in. H_2O Pressure drop through sample, wet-2.445 in. H_2O

Time (min.)	Moisture Content (lbs. moisture/lb. room dry sample %)	Drying Rate (lbs. moisture/ lb. room dry sample, min.)
0	149	0.21
1	129	0.16
2	116	0.15
3	103	0.13
4	89.5	0.125
5	76.2	0.12
6	63.0	0.10
7	54.5	0.08
8	49.5	0.06
9	43.0	0.06
10	36.5	0.06
11	33.0	0.06
12	26.4	0.05
13	20.0	0.045
14	16.6	0.040
15	13.2	0.035
16	9.9	0.032
17	6.64	0.030
18	3.32	0.025
19	2.00	0.020
20	0	0.010

Table 8. Data for Drying of Sample No. 3

Air Data: Tunnel Temperature, dry - 150°F.
Room Temperature, dry - 76°F.
Room Temperature, wet - 66°F.
Velocity, dry sample - 600 fpm

Sample Data: Sample No. 3 - See Table 1
Pressure drop through sample, dry-2.345 in. H_2O
Pressure drop through sample, wet-2.309 in. H_2O

Time (min.)	Moisture Content (lbs. moisture/lb. room dry sample %)	Drying Rate (lbs. moisture/ lb. room dry sample, min.)
0	273	1.52
0.25	241	1.12
0.50	213	0.92
0.75	196	0.80
1.00	178	0.80
1.25	157	0.80
1.50	138	0.80
1.75	119	0.80
2.00	98	0.80
2.25	77	0.80
2.50	56	0.78
2.75	38.5	0.64
3.00	24.5	0.52
3.25	10.5	0.40
3.50	3.5	0.28
3.75	0	0.12
4.00	0	0.02

Table 9. Data for Drying of Sample No. 1

Air Data: Tunnel Temperature, dry - 220°F.
Room Temperature, dry - 76°F.
Room Temperature, wet - 66°F.
Velocity, dry sample - 720 fpm

Sample Data: Sample No. 1 - See Table 1
Pressure drop through sample, dry-2.400 in. H_2O

Time (min.)	Moisture Content (lbs. moisture/lb. room dry sample %)	Drying Rate (lbs. moisture/ lb. room dry sample, min.)
0	340	5.0
0.20	275	3.2
0.40	222	2.2
0.60	175	1.60
0.80	147	1.13
1.00	131	0.90
1.20	110	0.90
1.40	91	0.90
1.60	78.2	0.90
1.80	59.4	0.90
2.00	43.7	0.65
2.20	34.4	0.50
2.40	25.0	0.44
2.60	15.6	0.35
2.80	9.38	0.25
3.00	6.25	0.15
3.20	3.13	0.10
3.40	0	0.05
3.60	0	0

Table 10. Data for Temperature Downstream to Sample

Air Data: Tunnel Temperature, dry - 148°F.
Room Temperature, dry - 75°F.
Room Temperature, wet - 66°F.
Velocity, dry sample - 790°F.

Sample Data: Sample No. 1 - See Table 1
Pressure drop through sample - 2.2880 in. H_2O

Time (sec.)	Temperature °F.	Time (sec.)	Temperature °F.
0	95	120	119
10	98	130	123
20	98	140	128
30	98	150	134
40	98	160	138
50	100	170	138
60	101	180	138
70	103	190	138
80	106	200	138
90	108	210	138
100	114	220	138
110	116	230	138

Table 11. Data for Temperature Downstream to Sample

Air Data: Tunnel Temperature - 77°F.
Room Temperature, dry - 76°F.
Room Temperature, wet - 64°F.
Velocity, dry sample - 655 fpm

Sample Data: Sample No. 3 - See Table 1
Pressure drop through dry sample-2.375 in. H_2O

Time (sec.)	Temperature °F.	Time (sec.)	Temperature °F.
0	66.6	310	73.7
10	70.0	320	73.8
20	70.0	330	73.8
30	70.7	340	74.0
40	70.7	350	74.0
50	71.4	360	74.2
60	71.8	370	74.3
70	71.8	380	74.4
80	71.8	390	74.5
90	71.8	400	74.5
100	71.8	410	74.7
110	72.5	420	74.8
120	72.5	430	74.8
130	72.5	440	74.9
140	73.2	450	74.9
150	73.2	460	75.0
160	73.2	470	75.0
170	73.2	480	75.2
180	73.2	490	75.2
190	73.3	500	75.4
200	73.3	510	75.6
210	73.3	520	75.6
220	73.4	530	75.8
230	73.4	540	75.8
240	73.5	550	76.0
250	73.5	560	76.0
260	73.6	570	76.0
270	73.6	580	76.0
280	73.6	590	76.0
290	73.6	600	76.0
300	73.7	610	76.0

Table 12. Data for Temperature Downstream to Sample

Air Data: Tunnel Temperature, dry - 203°F.
Room Temperature, dry - 76°F.
Room Temperature, wet - 66°F.
Velocity, dry sample - 644 fpm

Sample Data: Sample No. 4 - See Table 1
Pressure drop through dry sample-2.410 in. H_2O

Time (sec.)	Temperature °F.	Time (sec.)	Temperature °F.
0	71	250	137
10	84	260	138.5
20	87	270	140
30	94	280	142
40	98	290	145
50	98	300	147
60	102	310	149
70	105	320	153
80	106	330	158
90	107	340	158
100	109	350	162
110	111	360	162
120	111	370	165
130	115	380	165
140	117	390	165
150	119	400	165
160	122	410	165
170	123.5	420	165
180	125	430	169
190	127	440	169
200	128.5	450	169
210	130	460	169
220	132	470	169
230	133.5	480	169
240	135	490	169

Table 13. Data for Temperature Downstream to Sample

Air Data: Tunnel Temperature, dry - 183°F.
Room Temperature, dry - 75°F.
Room Temperature, wet - 66°F.
Velocity, dry sample - 646 fpm

Sample Data: Sample No. 4 - See Table 1
Pressure drop through dry sample-2.410 in. H_2O

Time (sec.)	Temperature °F.	Time (sec.)	Temperature °F.
0	90	90	172
10	98	100	174
20	98	110	176
30	98	120	178
40	110	130	180
50	122	140	182
60	142	150	182
70	155	160	182
80	165	170	182

Table 14. Data for Tuft Temperature*

Air Data: Tunnel Temperature, dry - 230°F.
Room Temperature, dry - 66°F.
Room Temperature, wet - 54°F.
Velocity, dry sample - 640 fpm

Sample Data: Sample No. 4 - See Table 1
Pressure drop through dry sample-2.4855 in. H_2O

Time (sec.)	Temperature °F.	Time (sec.)	Temperature °F.
0	73	110	205
10	90	120	215
20	91	130	216
30	92	140	217
40	94	150	222
50	95	160	225
60	102	170	228
70	115	180	228
80	135	190	228
90	162	200	228
100	185	210	228

*A thermocouple was buried in the short, uncut tuft of Sample No. 4. The bead of the thermocouple was located one-eighth of an inch from the jute backing.

Table 15. Data for Pressure Drop Through Carpet

Sample No.	Temperature °F. Room Duct	Dry	Wet	Velocity fpm	Pressure* Drop Carpet in.H_2O	Moisture Content %	Re**	C_f**
3	73	73	56	665	2.3165	0	432	0.700
3	73	73	56	630	2.2113	0	410	0.742
3	73	73	56	420	1.5000	0	274	1.135
3	73	73	56	240	0.8050	0	157	1.928
3	73	73	56	567	1.9796	0	368	0.822
3	73	73	56	495	1.7694	0	324	0.964
4	74	74	60	720	2.4000	0	502	0.610
4	74	74	60	700	2.3705	0	496	0.635
4	74	74	60	563	1.8910	0	400	0.778
4	74	74	60	460	1.3700	0	326	0.850
4	74	74	60	350	1.0716	0	249	1.145
1	80	75	58	785	2.2245	0	615	0.516
1	75	75	58	760	2.1400	0	595	0.529
1	75	75	58	575	1.5400	0	450	0.666
1	75	75	58	630	1.7630	0	494	0.635
1	72	70	58	595	1.6650	0	485	0.682
1	70	74	56	815	2.2824	0	625	0.550
3	220	73	56	600	2.3500	0	287	1.095
3	202	73	56	570	2.3500	0	256	1.239
3	202	73	56	534	2.2880	0	226	1.400
3	220	73	56	433	1.8105	0	187	1.662
3	220	73	56	330	1.2065	0	149	1.928
3	220	73	56	289	1.0380	0	124	2.160
3	170	73	56	600	2.3300	0	306	1.025
3	135	73	56	600	2.3250	0	328	0.994
3	105	73	56	600	2.3230	0	344	0.891
4	153	74	60	647	2.4265	0	360	0.765
4	185	74	60	646	2.4240	0	348	0.805
4	118	74	60	656	2.4270	0	340	0.890
3	73	73	64	655	2.3750	0	419	0.760
4	229	70	67	640	2.4850	0	285	1.042
4	200	70	67	644	2.4650	0	313	0.985
4	170	70	67	646	2.4530	0	340	0.940
1	279	71	64	694	2.4430	0	270	0.910
2	72	72	62	747	2.4425	0	497	0.594
3	150	76	66	600	2.3450	0	317	0.994
1	220	76	66	730	2.4000	0	356	0.861
1	148	75	66	790	2.2880	0	480	0.614

*The air was blown through from both sides of carpet. There was no measurable difference in the pressure drop.

**See Equations (10) and (13), Chapter III, for derivations.

Table 16. Comparison of Analytical and Experimental Drying Time and Rates.

Sample No.	Data from Table No.	Constant Drying Rate (lbs. moisture evp'd/lb. room dry sample, min.)		Drying Time During Falling Rate Period (min.)	
		Exper.	Eqn. (27)	Exper.	Eqn. (34)
1	2	0.250	0.190	8.0	10.8
1	3	1.560	1.750	0.835	0.943
2	4	0.170	0.173	3.00	3.47
3	5	0.180	0.164	4.50	5.12
4	6	0.520	1.320	2.20	1.41
3	8	0.800	0.900	1.40	1.83
1	9	0.900	1.250	1.88	1.44

APPENDIX F

ESTIMATED ERRORS

Flow Rate

It was estimated that the maximum deviation from average measurement of the flow rate was plus or minus 50 cfm, occurring at 800 cfm. This was observed by the manometer fluctuation. The deviation in the flow rate when running the sample on different days was a maximum of 70 cfm at 800 cfm giving a maximum error of 9 per cent. It appeared that slightly different flow patterns were set up through the carpet on each occasion.

Temperature

The maximum deviation in temperature measurement was plus or minus 10°F. at 250°F., giving a maximum variation of 4 per cent, as observed from the recorder. The transit time required for the system to reach operating temperature for temperatures above 250°F. caused an error in the average temperatures during the drying test of minus 30°F., giving a maximum error of 10 per cent. This transit error was determined by recording the initial temperature at the start of dryer, the time to reach operating condition, and the total time. Using this data the average temperature and deviation was determined.

Pressure Differential

The maximum fluctuation in pressure differential

was plus or minus 0.004 inches H_2O at 2.2830 inches H_2O. This gave a maximum possible error of 0.18 per cent. The deviation was determined by the same procedure used in determining errors in flow rate measurements.

Drying Weight

The maximum fluctuation in drying weight was plus or minus 0.03 pounds for a weight change of 0.50 pounds. This gave a maximum possible error of 3/50 or 6 per cent. The error occurred in the drying of samples at high temperatures, due to the inability to maintain a constant temperature in the weighing section. The error was due to the effect of the temperature on the strain gages in the weighing section. The maximum deviation was determined by running a dry sample at various temperatures and recording the change caused by the temperature variations.

Time

It was estimated that the maximum possible error in stopping and starting the chart drives on the recorders was plus or minus 2 seconds in a period of 60 seconds. This gave a maximum possible error of 3.33 per cent. The error was determined by comparing the times indicated on the charts of the recorders with that on a stop watch.

It was estimated that the error in determining the exact drying time was plus or minus 10 seconds in 60 seconds or about 17 per cent. This was due to diffusion of moisture

from the unexposed area in the weighing frame which indicated that drying was still occurring on the weight recorder. This diffusion can be observed by the final drops in the rate-of-drying curves.

Reproducibility of Experimental Results

The samples were dried under identical conditions on different days. Slightly different flow rates were measured due to different flow patterns being set up through the carpet. The drying rates and times could be reproduced within 10 per cent on all samples except runs at temperatures above 260°F. For these runs the time varied as much as 50 per cent depending on the temperature of the drying and transit time required to reach operating conditions.

APPENDIX G

BIBLIOGRAPHY

BIBLIOGRAPHY

Literature Cited

1. Bell, J. R. and Grosberg, P., "The Movement of Vapor and Moisture During the Falling Rate Period of Drying of Thick Textile Materials," Journal of the Textile Institute, Vol. 53, No. 5, 1962, p. 250.

2. Carman, P. C., "Fluid Flow Through Granular Beds," Transactions of the Institution of Chemical Engineers, Vol. 15, 1937, p. 150.

3. Carrier, W. H., "The Theory of Atmospheric Evaporation," Industrial and Engineering Chemistry, Vol. 13, No. 5, 1921, p. 432.

4. Cassie, A. B. D., "Propagation of Temperature Changes Through Textiles in Humid Atmospheres." Part II - "Theory of Propagation of Temperature Change," Transactions of the Faraday Society, Vol. 35, 1940, pp. 453-458.

5. Cassie, A. B. D., "Propagation of Temperature Changes Through Textiles in Humid Atmospheres," Part III - "Experimental Verification of Theory," Transactions of the Faraday Society, Vol. 35, 1940, pp. 458-465.

6. Kreith, Frank, Principles of Heat Transfer, International Textbook Co., Scranton, Penn., 1958.

7. Lewis, W. K., "The Rate of Drying Solids Materials," Industrial and Engineering Chemistry, Vol. 13, No. 5, 1921, p. 427.

8. Lord, Joan, "The Determination of the Air Permeability of Fabrics," The Journal of the Textile Institute, Vol. 50, 1959, p. 569.

9. McCready, Donald W. and McCabe, Warren L., "The Adiabatic Air Drying of Hygroscopic Solids," Transactions of the American Institute of Chemical Engineers, Vol. 29, 1933, p. 131.

10. McMahon, G. B. and Downes, J. G., "Propagation of Temperature and Moisture Changes During Forced Convective Flow of Air Through a Mass of Hygroscopic Fibers," International Journal of Heat Mass Transfer, Vol. 5, 1962, pp. 689-696.

11. Newman, Albert B., "The Drying of Porous Solids," Transactions of American Institute of Chemical Engineers, Vol. 27, 1931, p. 203, 310.

12. Perry, John H., "The Drying of Solids," Chemical Engineers' Handbook, McGraw-Hill Book Company, Inc., New York, N. Y., 1950, p. 806.

13. Sherwood, T. K., "The Drying of Solids - I," Industrial and Engineering Chemistry, Vol. 21, No. 1, 1929, p. 12.

14. Sherwood, T. K., "The Drying of Solids - II," Industrial and Engineering Chemistry, Vol. 21, No. 10, 1929, p. 976.

15. Sherwood, T. K., "The Drying of Solids - III," Industrial and Engineering Chemistry, Vol. 22, No. 2, 1930, p. 132.

16. Trebal, Robert E., "Drying," Mass-Transfer Operations, McGraw-Hill, New York, 1955, pp. 524-579.

Other References

Encyclopedia of Textiles, Prentice-Hall, Inc., Englewood Cliffs, N. J., p. 603.

Matthews, J. Merritt, The Textile Fibers, Their Physical Microscopical and Chemical Properties, John Wiley & Sons, Inc., New York, N. Y., 1936, p. 102.

Strock, Clifford, Editor, Handbook of Air Conditioning, Heating and Ventilating, The Industrial Press, New York, N. Y., 1959, pp. 1-72.

Textile World, "Manufacturing," Fact File Issue Mid-July, 1960, Vol. 110, No. 7, p. 60.

Textile World, "Man Made Fiber Chart," Fact File Issue Mid-July, 1962, Vol. 112, No. 7, P. 158.